

PROBING THE ISM NEAR STAR FORMING REGIONS WITH GRB AFTERGLOW SPECTROSCOPY: GAS, METALS, AND DUST

JASON X. PROCHASKA¹, HSIAO-WEN CHEN², MIROSLAVA DESSAUGES-ZAVADSKY³, JOSHUA S. BLOOM⁴

Submitted to ApJ; March 2 2007

ABSTRACT

We study the chemical abundances of the interstellar medium surrounding high z gamma-ray bursts (GRBs) through analysis of the damped Ly α systems (DLAs) identified in afterglow spectra. These GRB-DLAs are characterized by large H I column densities N_{HI} and metallicities $[\text{M}/\text{H}]$ spanning 1/100 to nearly solar, with median $[\text{M}/\text{H}] > -1$ dex. The majority of GRB-DLAs have $[\text{M}/\text{H}]$ values exceeding the cosmic mean metallicity of atomic gas at $z > 2$, i.e. if anything, the GRB-DLAs are biased to larger metallicity. We also observe (i) large $[\text{Zn}/\text{Fe}]$ values ($> +0.6$ dex) and sub-solar Ti/Fe ratios which imply substantial differential depletion, (ii) large α/Fe ratios suggesting nucleosynthetic enrichment by massive stars, and (iii) low C^0/C^+ ratios ($< 10^{-4}$). Quantitatively, the observed depletion levels and C^0/C^+ ratios of the gas are not characteristic of cold, dense H I clouds in the Galactic ISM. We argue that the GRB-DLA represents the ISM near the GRB but not gas directly local to the GRB (e.g. its molecular cloud or circumstellar material). We compare these observations with DLAs intervening background quasars (QSO-DLAs). The GRB-DLAs exhibit larger N_{HI} values, higher α/Fe and Zn/Fe ratios, and have higher metallicity than the QSO-DLAs. Although these differences are statistically significant, the offsets are relatively modest (N_{HI} excepted). We argue that the differences primarily result from galactocentric radius-dependent differences in the ISM: GRB-DLAs preferentially probe denser, more depleted, higher metallicity gas located in the inner few kpc whereas QSO-DLAs are more likely to intersect the less dense, less enriched, outer regions of the galaxy. Finally, we investigate whether dust obscuration may exclude GRB-DLA sightlines from QSO-DLA samples; we find that the majority of GRB-DLAs would be recovered which implies little observational bias against large N_{HI} systems.

Subject headings: quasars : absorption lines

^aDepartment of Astronomy and Astrophysics, UCO/Lick Observatory; University of California, 1156 High Street, Santa Cruz, CA 95064; xavier@ucolick.org

^bDepartment of Astronomy; University of Chicago; 5640 S. Ellis Ave., Chicago, IL 60637; hchen@oddjob.uchicago.edu

^cObservatoire de Genève, 51 Ch. des Maillettes, 1290 Sauverny, Switzerland

^dDepartment of Astronomy, 601 Campbell Hall, University of California, Berkeley, CA 94720-3411

1. INTRODUCTION

For the past decade, high resolution spectroscopy of distant quasars (QSOs) have enabled detailed studies of the chemical abundances of high z galaxies (e.g. Lu *et al.* 1996; Prochaska & Wolfe 1999; Dessauges-Zavadsky *et al.* 2001; Molaro *et al.* 2001; Prochaska *et al.* 2001; Ledoux, Petitjean & Srianand 2003). These properties of the interstellar medium (ISM) have been surveyed extensively via the damped Ly α systems (DLAs), galaxies intersected by sightlines to distant quasars (for a review, see Wolfe, Gawiser & Prochaska 2005). These QSO-DLA sightlines sample galaxies according to gas cross-section, i.e. the outer regions of a galaxy's ISM are more frequently probed because differential cross-section is proportional to radius. If star formation (SF) occurs in compact regions in high z galaxies (i.e. molecular clouds), then QSO-DLAs would only rarely probe these environments (Zwaan & Prochaska 2006). This conclusion holds true independent of any additional biases related to dust obscuration by the SF regions themselves (e.g. Fall & Pei 1993). QSO-DLA surveys are an inefficient approach to directly studying the gas in high z SF regions.

Like quasars, gamma-ray bursts (GRBs) provide a bright – albeit transient – light beam from the distant universe. Imprinted on the roughly power-law spectrum of the afterglow are the signatures of the intergalactic medium (e.g.

Fiore *et al.* 2005; Chen *et al.* 2005; Prochter *et al.* 2006) and transitions from the ISM surrounding the GRB event (e.g. Savaglio, Fall & Fiore 2003; Vreeswijk *et al.* 2004; Prochaska *et al.* 2006). And, analogous to absorption line studies of quasars, these observations reveal the H I column density (Vreeswijk *et al.* 2004; Jakobsson *et al.* 2006), metallicity (Fynbo *et al.* 2006; Prochaska 2006), chemical abundances, differential depletion (Savaglio & Fall 2004), and kinematics (Paper II; Prochaska *et al.* 2007) of the gas along the sightline.

The progenitors of long-duration GRB are believed to be massive stars residing in active star forming regions (Woosley 1993; Woosley & Bloom 2006). At low redshift, this association is well established: supernova have been identified at the same position as GRB events (e.g. Hjorth *et al.* 2003; Stanek *et al.* 2003; Mirabal *et al.* 2006, but see also Fynbo *et al.* (2006)). Furthermore, GRBs have been found recently to be located within Wolf-Rayet galaxies (Hammer *et al.* 2006). The connection between GRB and star-forming regions is inferred at high redshift. GRBs are found exclusively in galaxies that are blue and show nebular emission lines indicative of ongoing star formation (Le Floch *et al.* 2003). Furthermore, high precision astrometry of long-duration GRB afterglows reveal these events occur exclusively within 10 kpc of the flux-weighted centroid of their

host galaxy (Bloom, Kulkarni & Djorgovski 2002; Fruchter *et al.* 2006). Therefore, the sightlines to GRBs should probe the ISM within or at least near star-forming regions. In this respect, studies of the ISM along sightlines to GRBs complement those toward quasars.

The first observations of GRB-DLAs indicated large H I column density (Castro *et al.* 2003; Vreeswijk *et al.* 2004) and large metal-line equivalent widths and column densities (Metzger *et al.* 1997; Savaglio, Fall & Fiore 2003). These data suggested modestly enriched gas ($\gtrsim 1/10$ solar) and substantial depletion levels but the analysis is limited by line-saturation (i.e. low-resolution spectroscopy of lines with large optical depth; Prochaska 2006). With the launch of the Swift satellite (Gehrels 2000), GRBs are detected at a rate of ≈ 2 per week with rapid, precise localizations enabling echelle observations of a modest sample of GRB-DLAs (Chen *et al.* 2005; Prochaska, Chen & Bloom 2006; Vreeswijk *et al.* 2006; Prochaska *et al.* 2006; Piranomonte *et al.* 2007). These observations provide precise column density measurements of many metal-line transitions and permit the analysis of the chemical abundances in the gas surrounding GRB.

In this paper, we describe the chemical abundances of a modest sample of damped Ly α systems associated with the ISM surrounding gamma-ray bursts. We focus on echelle observations acquired in the past two years, but also include pre-Swift observations. Our principal goal is to describe the physical conditions of the interstellar medium within and/or near star formation regions in the young universe. To frame the discussion, we will compare the GRB-DLA observations against similar sets of observations for damped Ly α systems along quasar sightlines (QSO-DLAs).

There are at least three reasons why one may expect the ISM characteristics of the GRB-DLAs to differ with those of QSO-DLAs. First, the two samples may arise from overlapping yet non-identical populations of high z galaxies. By definition, the QSO-DLAs correspond to galaxies with large H I surface densities. These are selected independently of any emission or stellar property (Wolfe *et al.* 1986) and cosmological simulations suggest a subset may not even be located within dark matter halos (Razoumov *et al.* 2006). Long-duration GRB, in contrast, are known to occur only within star-forming galaxies and are expected to roughly trace the on-going star formation rate (SFR; e.g. Totani 1999; Ramirez-Ruiz, Trentham & Blain 2002; Guetta & Piran 2007). Of course, star-forming galaxies presumably also have large H I column densities⁵, as evidenced by the DLA profiles in GRB afterglows.

Second, even if QSO-DLAs and GRB-DLAs are drawn from the exact same parent population of host galaxies, the QSO-DLAs are selected according to H I covering fraction on the sky while GRB are expected to track current SFR. One may expect QSO-DLA to preferentially arise in galaxies with extended H I disks (e.g. low-surface brightness) whereas GRB preferentially occur within high-surface brightness galaxies (Mo, Mao & White 1998). Finally, and perhaps the most important, QSO-DLAs will

preferentially probe the outer regions of galaxies whereas GRB-DLAs are generally located within the inner few kpc of their host galaxies (Bloom, Kulkarni & Djorgovski 2002). This could imply higher N_{HI} values, metallicity, depletion levels, molecular fractions, and differential rotation along the GRB-DLAs sightlines. Therefore, a secondary theme of this paper is to test the hypothesis that GRB-DLAs and QSO-DLAs are drawn from the same parent population of high z galaxies and that any differences in ISM properties are explained by their average impact parameters through the galaxies.

This paper is organized as follows. Section 2 presents the experimental design, and observational samples. In § 3, we characterize the H I column densities, metallicities, relative abundances, and atomic carbon abundance of GRB-DLAs. We discuss the implications of these results in § 4 and conclude with a list of future directions.

2. EXPERIMENTAL DESIGN AND OBSERVATIONAL SAMPLES

2.1. Sightline Geometries

Before discussing the observational data, it is important to comment further on a few fundamental differences between studying DLAs along GRB sightlines versus background QSOs. The most obvious differences are that the GRB sightline originates within the galaxy giving rise to the damped Ly α system and, almost certainly, from within a young star-forming region. This implies several important consequences for the DLAs probed by GRB afterglows.

First, because the phenomena originates from within the DLAs themselves, a GRB sightline intersects less gas column than a background QSO sightline would at the same position on the sky. Therefore, one underestimates the average H I column density and may underestimate the total velocity field that occurs along the sightline. Second, it is possible that gas local to the progenitor, i.e. circumstellar material and/or molecular cloud gas, contributes significantly to the GRB-DLAs (but see below). One may expect especially large dust-to-gas ratios, high molecular fractions, and/or peculiar chemical abundance ratios. Third, the GRB afterglow radiation can significantly affect the DLAs observed along its sightline whereas QSO-DLAs are selected to have large distance from their background QSO. The UV flux from a GRB afterglow that is typical of spectroscopic observations (i.e. peak magnitude of $R \approx 15$ at early times) is sufficient to ionize an H I column of approximately 10^{21} cm^{-2} at 5 pc from the afterglow in only a few minutes time (e.g. Draine & Hao 2002; Perna & Lazzati 2002; Prochaska, Chen & Bloom 2006). Similarly, theoretical treatments predict the X-ray and UV components of the afterglow can destroy dust and molecular hydrogen out to 10 to 100 pc (Waxman & Draine 2000; Fruchter, Krolik & Rhoads 2001; Draine & Hao 2002). If neutral gas and dust existed at distances of ~ 10 pc prior to the burst, it is likely removed by the afterglow before spectroscopic observations are initiated. In this respect, the contribution of gas local to the GRB is somewhat minimized by the GRB event itself. By the same token, gas local to the star forming regions may have been attenuated by the afterglow radiation field and our observations may not precisely reflect the conditions of this gas in the

⁵Similarly, we may expect that all galaxies with large H I column density will exhibit star formation. Indeed, the presence of heavy elements in all QSO-DLAs indicates previous star formation (Prochaska *et al.* 2003) and C II* fine-structure absorption implies ongoing star formation (Wolfe, Prochaska & Gawiser 2003).

TABLE 1
GRB-DLA SAMPLE

GRB	RA	DEC	z_{GRB}	Instrument	R	Mg I ^a	Exc. Fe II ^b	Ref
GRB990123	15:25:30.34	+44:45:59.1	1.600	Keck/LRIS	1,000	Y	N	1
GRB000926	17:04:09.00	+51:47:10.0	2.038	Keck/ESI	5,000	Y	N	2
GRB010222	14:52:12.55	+43:01:06.2	1.477	Keck/ESI	5,000	Y	N	3
GRB011211	11:15:17.98	-21:56:56.2	2.142	VLT/FORS2	1,000	?	N	1,4
GRB020813	19:46:41.87	-19:36:04.8	1.255	Keck/LRIS	1,000	Y	Y	5
GRB030226	11:33:04.93	+25:53:55.3	1.987	Keck/ESI	5,000	?	N	6
GRB030323	11:06:09.40	-21:46:13.2	3.372	VLT/FORS2	1,000	Y	N	7
GRB050401	16:31:28.82	+02:11:14.8	2.899	VLT/FORS2	1,000	?	N	8
GRB050505	09:27:03.20	+30:16:21.5	4.275	Keck/LRIS	1,000	?	N	9
GRB050730	14:08:17.14	-03:46:17.8	3.969	Magellan/MIKE	30,000	?	Y	10
GRB050820	22:29:38.11	+19:33:37.1	2.615	Keck/HIRES	30,000	N	N	11
GRB050904	00:54:50.79	+14:05:09.4	6.296	Subaru/FOCAS	1,000	?	?	12
GRB050922C	19:55:54.48	-08:45:27.5	2.199	VLT/UVES	30,000	W	Y	13
GRB051111	00:08:17.14	-00:46:17.8	1.549	Keck/HIRES	30,000	Y	Y	14,11
GRB060206	13:31:43.42	+35:03:03.6	4.048	WHT/ISIS	4,000	?	?	15
GRB060418	15:45:42.40	-03:38:22.80	1.490	Magellan/MIKE	30,000	Y	Y	11

^aStrong MgI absorption (W=weak). GRB-DLA with strong Mg I absorption are likely to have the majority of their gas at distances greater than 50pc from the afterglow (Prochaska, Chen & Bloom 2006)

^bPositive detection of absorption from excited levels of Fe⁺. This measurement is difficult in low-resolution data and a non-detection should be interpreted as ambiguous. The absence of absorption in higher resolution data, however, indicates the Fe⁺ gas (observed via resonance lines) is at large distance from the afterglow.

References. — 1: Savaglio, Fall & Fiore (2003); 2: Castro *et al.* (2003); 3: Mirabal *et al.* (2002); 4: Vreeswijk *et al.* (2006); 5: Barth *et al.* (2003); 6: Shin *et al.* (2006); 7: Vreeswijk *et al.* (2004); 8: Watson *et al.* (2006); 9: Berger *et al.* (2006); 10: Chen *et al.* (2005); 11: Prochaska *et al.* (2006); 12: Kawai *et al.* (2006); 13: Piranomonte *et al.* (2007); 14: Prochaska, Chen & Bloom (2006); 15: Fynbo *et al.* (2006)

absence of a GRB.

On the other hand, aside from the UV pumping of fine-structure lines (Prochaska, Chen & Bloom 2006; Dessauges-Zavadini *et al.* 2006; Vreeswijk *et al.* 2006), there is no compelling case of a GRB afterglow having attenuated its surrounding medium. There have been no substantiated reports of line variability in any resonance line including, and most importantly, Mg I transitions. The majority of GRB-DLAs exhibit strong Mg I absorption coincident in velocity with the resonance and excited transitions of low-ion species (Prochaska, Chen & Bloom 2006; Prochaska *et al.* 2006). This atom has an ionization potential IP=7.7 eV and would be ionized by the afterglow if it occurs within ≈ 100 pc of the event. Prochaska, Chen & Bloom (2006) have argued, therefore, that the majority of neutral gas observed in GRB-DLAs is at a distance exceeding 100 pc from the progenitor. Meanwhile, the detection of UV pumped excited states of Si⁺, O⁰, and Fe⁺ require that the gas is located within ≈ 1 kpc of the afterglow. Indeed, Vreeswijk *et al.* (2006) have analyzed variations in the level populations of the excited levels of Fe⁺ and Ni⁺ and constrain the distance of the GRB-DLAs along the GRB 060418 sightline to be at 1 ± 0.2 kpc from the afterglow.

Table 1 indicates those GRB-DLAs that exhibit strong Mg I absorption. We also identify the GRB-DLAs which show absorption from excited states of Fe⁺. Those cases without Fe⁺ fine-structure absorption must also lie at distances $\gtrsim 100$ pc (Prochaska, Chen & Bloom 2006; Chen *et al.* 2007). These results indicate that the majority of gas in GRB-DLAs is not local to the star formation region and should not be adversely affected by the GRB afterglow. Our current expectation is that O and B stars from the

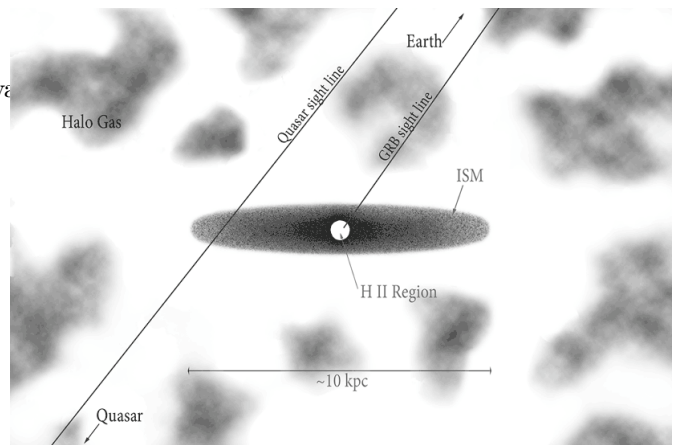


FIG. 1.— This cartoon illustrates the likely differences between QSO-DLA and GRB-DLA sightlines. The former have randomly intersected a foreground galaxy. These QSO-DLA sightlines correspond to a cross-section selected sample and should preferentially intersect the outer regions of the ISM in high z galaxies. In contrast, the GRB-DLAs are constrained to originate from within the ISM of their host galaxies, presumably the H II region produced by massive stars in a star-forming region. These GRB-DLA sightlines are expected (and observed) to originate within the inner few kpc of the ISM.

star-forming region have ionized all gas within ≈ 100 pc of the GRB producing large H II regions. Figure 1 presents a cartoon illustration of a GRB and a QSO sightline through a galaxy comprised of a neutral ISM surrounded by predominantly ionized halo gas clouds. The GRB sightline originates near the center of the galaxy, within an H II region associated with ongoing star-formation. In contrast,

TABLE 2
QSO-DLA SAMPLES

Sample	Description	N_{DLA}	Instrument(s)	Ref
HR-A	High-resolution full sample (all)	153	HIRES, ESI, UVES	1,2,3,4,5
HR-S	High-resolution ‘statistical’ sample	112	HIRES, ESI, UVES	5
HR-E	High precision echelle	71	HIRES, UVES	1,2
SDSS	True (N_{HI}) statistical sample	475	SDSS	6,7

References. — 1: Prochaska *et al.* (2007); 2: Dessauges-Zavadsky *et al.* (2006); 3: Ledoux *et al.* (2006); 4: Herbert-Fort *et al.* (2006); 5: Prochaska *et al.* (2003); 6: Prochaska & Herbert-Fort (2004); 7: Prochaska, Herbert-Fort & Wolfe (2005)

the QSO-DLA sightlines will preferentially penetrate the outer regions of the ISM.

Independent of the differences one may expect for QSO-DLAs and GRB-DLAs, there may be common trends (e.g. metallicity vs. dust depletion) characteristic of the ISM of all high z galaxies. By considering the QSO-DLAs and GRB-DLAs together, we hope to reveal these global trends in addition to highlighting differences in the samples.

2.2. GRB-DLA and QSO-DLA Samples

The QSO-DLA samples are drawn from two sources: (i) high-resolution echelle and echellette observations of quasars acquired with the HIRES (Vogt *et al.* 1994) and ESI (Sheinis *et al.* 2000) spectrometers at the Keck Observatory and the UVES (Dekker *et al.* 2000) spectrometer at the VLT Observatory; and (ii) the low-resolution QSO-DLA surveys of the Sloan Digital Sky Survey (SDSS; Prochaska & Herbert-Fort 2004; Prochaska, Herbert-Fort & Wolfe 2005). We will restrict the samples to $z_{\text{DLA}} > 1.6$ and DLAs which are greater than 3000 km s^{-1} from their background quasar. The high-resolution sample (HR-A) is summarized in these papers: Herbert-Fort *et al.* (2006); Ledoux *et al.* (2006); Dessauges-Zavadsky *et al.* (2006); Prochaska *et al.* (2007). Prochaska *et al.* (2007) have emphasized that the full dataset is a heterogeneous sample of QSO-DLAs including a number of systems selected on the basis of strong metal-lines (Herbert-Fort *et al.* 2006) or as promising candidates for H_2 absorption (Ledoux, Petitjean & Srianand 2003). As such, the H I distribution $f(N_{\text{HI}})$ of the high-resolution sample does not follow the statistical distribution derived from the SDSS.

For a number of the comparisons made in this paper, we will take subsets of these samples. In particular, we define a pseudo-statistical sample of metallicity measurements (HR-S) which is restricted to the compilation of Prochaska *et al.* (2003). We also construct a sample of high quality echelle-only observations (HR-E) for analysis related to relative abundances (e.g. α/Fe). The echellette observations, in particular, have too poor data quality to generally achieve better than 0.1 dex precision (Prochaska *et al.* 2003) and are not included. Although the DLAs in these high-resolution subsets do not follow $f(N_{\text{HI}})$ for a random sample, they were selected only on the basis of a large H I column density. Table 2 summarizes the various QSO-DLA samples considered in this paper.

Our selection criteria for the GRB-DLA sample are (i) the presence of a damped $\text{Ly}\alpha$ system ($N_{\text{HI}} \geq 2 \times 10^{20} \text{ cm}^{-2}$) or a low-ion column density that requires N_{HI} exceed $2 \times 10^{20} \text{ cm}^{-2}$

assuming solar metallicity⁶; (ii) spectra with sufficient signal-to-noise and resolution to study the chemical abundances of the gas. The sample is also limited to GRB-DLAs where we could access the data or where precise equivalent width measurements were reported in the literature. Table 1 lists the GRB-DLAs comprising our sample and describes the spectral observations.

As with QSO-DLAs (Fall & Pei 1993), it is likely that dust obscuration plays a role in defining the GRB-DLA sample. There are several examples in the literature of highly reddened afterglows which are likely extinguished by dust in the GRB host galaxy (e.g. Levan *et al.* 2006; Pellizza *et al.* 2006). At present, no comprehensive study on the incidence of optically ‘dark’ bursts has been performed nor an evaluation of the fraction of dark bursts which are cases of dust obscuration (as opposed to high z events). We expect, however, that dust obscuration is important to defining GRB-DLA samples.

2.3. Absorption-Line Metallicities

Metallicity is the mass density in metals relative to hydrogen and helium gas. It is likely that oxygen dominates this quantity in nearly every astrophysical environment, with carbon and nitrogen secondary. Although these three elements exhibit low-ion transitions, the majority are either too strong, too weak, and/or located within the $\text{Ly}\alpha$ forest. Therefore, the metal abundance of the interstellar medium is frequently gauged by other elements. Unfortunately, many of the transitions which are accessible to analysis arise from elements that are refractory. To avoid the complications of depletion corrections (which can be an order of magnitude or more), observers have focused on non-refractory or mildly refractory elements. These include S, Si, and Zn. The latter is a trace element, $\log(\text{Zn}/\text{H})_{\odot} = -7.3$, with an uncertain nucleosynthetic origin (Hoffman *et al.* 1996) and, therefore, should be considered cautiously.

A point of great interest in GRB studies is the metallicity of the progenitor especially in the context of the collapsar model (Woosley 1993). In the collapsar paradigm, large angular momentum is required to power the GRB. Because high metallicity stars are expected to have significant mass-loss by winds promoting the loss of angular momentum (Vink & de Koter 2005), Langer & Norman (2006) and Woosley & Heger (2006) have argued that GRB pro-

⁶We note that the few GRB sightlines with $N_{\text{HI}} < 10^{20} \text{ cm}^{-2}$ have very low column densities for low-ion transitions (Fiore *et al.* 2005; Prochaska *et al.* 2005).

genitors will have low metallicity, i.e. less than 1/10 solar abundance. One may consider this to be a natural prediction of the collapsar model.

There is at least circumstantial evidence in support of a metallicity ‘bias’ from studies of $z < 1$ GRB host galaxies. The metallicities of the H II regions in a small sample of $z < 0.5$ galaxies hosting GRBs are sub-solar (Prochaska *et al.* 2004; Sollerman *et al.* 2005) and several authors have noted that the values are systematically lower than the predicted distribution for galaxies drawn randomly according to current SFR (Stanek *et al.* 2006; Kewley *et al.* 2007; Modjaz *et al.* 2007). Furthermore, the GRB host galaxies at $z \sim 1$ are generally sub- L_* consistent with low metallicity (Le Floc’h *et al.* 2003). Fruchter *et al.* (2006) compared a sample of $z \lesssim 1$ GRB host galaxies against the host population for core-collapse supernova and demonstrated that GRB host galaxies have systematically lower luminosity. The difference is approximately one magnitude which they suggested could be due to a metallicity bias. However, galaxies follow a metallicity-luminosity relation that is roughly linear (Kobulnicky & Kewley 2004) and a one magnitude difference in luminosity implies only an approximately 0.3 dex offset in metallicity. Recently, Wolf & Podsiadlowski (2006) performed a thorough analysis showing the observations suggest a metallicity ‘ceiling’ for GRB progenitors but that this cutoff occurs at no lower than 1/2 solar. Therefore, while the offset in luminosities between the host galaxies of GRB and core-collapse supernova may be explained by a metallicity bias, this does not imply as severe an effect as promoted by studies of mass-loss.

At high redshift, it is difficult to observe nebular lines to measure metallicities and our knowledge of galaxies is too poor to make robust statements from luminosity distributions alone. Instead, one can measure the metallicity of the interstellar medium from absorption-line spectroscopy by comparing the total hydrogen column density with the total column density of metals.

3. GAS PHASE ABUNDANCES IN GRB-DLAs

In this section, we present column densities of hydrogen and metals observed in the gas-phase in GRB-DLAs. These observations give the surface density and metallicity of the ISM, and the relative abundances reflect differential depletion and the underlying nucleosynthetic patterns in the gas. Finally, we comment on the abundance of atomic carbon. In all of this analysis, we draw comparisons between the GRB-DLAs and QSO-DLAs.

3.1. Hydrogen Column Densities

In principle, the absorption-line spectra of rest-frame UV transitions ($\lambda < 3000\text{\AA}$) will give measurements of the atomic hydrogen and molecular hydrogen column densities, N_{HI} and N_{H_2} . For a damped Ly α system, the former is best determined through a Voigt profile fit to the Ly α $\lambda 1215$ transition. At $N_{\text{HI}} > 10^{20} \text{ cm}^{-2}$, the damping wings of the Lorentzian line-profile are well-resolved with a moderate resolution spectrum ($\text{FWHM} < 5\text{\AA}$). Therefore, aside from the redshift, the N_{HI} value is the most readily measured physical characteristic of a damped Ly α system.

Figure 2 presents the sample of N_{HI} measurements for our GRB-DLA sample supplemented by the compilation of Jakobsson *et al.* (2006) and compared against the distribution of N_{HI} values for QSO-DLAs measured from the

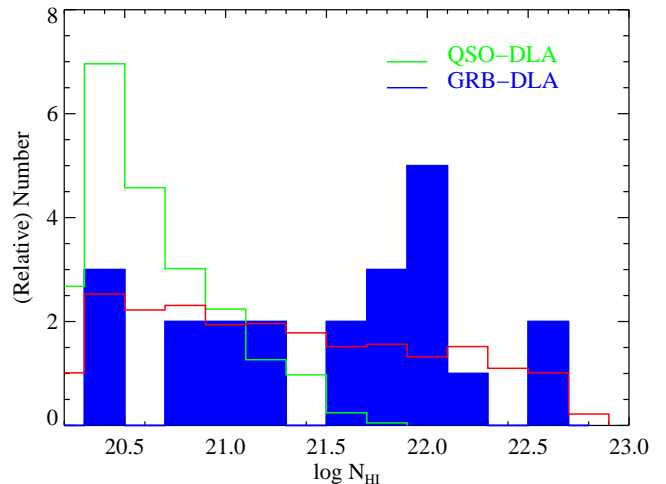


FIG. 2. — Blue (dark, solid) curve traces the histogram of N_{HI} values for the GRB-DLAs. In comparison, we show a histogram of N_{HI} values for QSO-DLAs drawn randomly toward background quasars (Prochaska, Herbert-Fort & Wolfe 2005) and normalized for presentation to have the same number of systems as the GRB-DLA sample. The GRB-DLAs have median value $\log N_{\text{HI}} = 21.7$, which exceeds all but a few QSO-DLAs observed to date. The dotted red line traces the predicted distribution of N_{HI} values assuming a sample of sightlines originating inside an H II region located at the center of an H I exponential disk. The model shown has central column density $\log N_0 = 22$, scale-height to scale-radius $h/R = 0.1$, and an H II region with radius $r_{\text{HII}} = 4h$.

Sloan Digital Sky Survey (Prochaska, Herbert-Fort & Wolfe 2005). As previously reported (Vreeswijk *et al.* 2004; Jakobsson *et al.* 2006), the GRB-DLA distribution is skewed to significantly higher N_{HI} values than QSO-DLAs. The difference, at least qualitatively, supports the hypothesis that QSO-DLAs probe the outer regions of galaxies whereas GRB-DLAs probe the inner, star-forming regions. Jakobsson *et al.* (2006) discussed that the GRB-DLA distribution is roughly consistent with that predicted for GRB embedded within molecular clouds (Reichart & Price 2002). The authors note, however, that GRB exhibit too many sightlines with $N_{\text{HI}} < 10^{22} \text{ cm}^{-2}$ compared to the prediction for molecular clouds. They argue this may result from photoionization and/or because GRB are preferentially located at the edge (White *et al.* 1999) or even outside molecular clouds (Hammer *et al.* 2006).

As we discussed in § 2.1, however, the presence of strong Mg I absorption in nearly every GRB sightline argues that the majority of GRB-DLA gas is located beyond $\approx 100\text{pc}$ of the event. This distance is comparable to only the largest giant molecular cloud complexes in the Local Group (Blitz *et al.* 2007) and it is reasonable to assume that the GRB-DLA gas is generally not associated with the molecular cloud hosting the GRB (see § 4.1). Examining Figure 2 in this light, the most salient question becomes: why do GRB-DLAs exhibit a preponderance of $N_{\text{HI}} > 10^{22} \text{ cm}^{-2}$ measurements? Indeed, the gas mass required to average $N_{\text{HI}} = 10^{22} \text{ cm}^{-2}$ at 100 pc along random sightlines is $M_{\text{HI}} = 10^7 M_{\odot}$; this exceeds the masses of even the largest molecular clouds in the Milky Way (Solomon & Rivolo 1989; Blitz 1993). It seems unlikely, therefore, that the observed H I gas corresponds to the

TABLE 3
GRB-DLA ABUNDANCE SUMMARY

GRB	$\log N_{\text{HI}}$	f_{α}^a	$[\alpha/\text{H}]$	$\sigma(\alpha)^b$	f_{Zn}^c	$[\text{Zn}/\text{H}]$	$\sigma(\text{Zn})^b$	f_M^d	$[\text{M}/\text{H}]$	$\sigma(\text{M})^b$	f_{Fe}^e	$[\text{Fe}/\text{H}]$	$\sigma(\text{Fe})^b$	$[\text{Ti}/\text{H}]^f$	f_{N}^g	$[\text{N}/\text{H}]$	$\sigma(\text{N})$	$N(\text{C}^0)^g$
GRB990123	22^a	0			2	-0.97	L.L.	12	-0.97	L.L.	2	-2.00	L.L.		0			
GRB000926	$21.30^{+0.25}_{-0.25}$	2	-1.58	L.L.	1	-0.17	0.15	2	-0.17	0.29	5	-1.49	0.08	-0.43	0			13.9
GRB010222	22^a	2	-1.61	L.L.	2	-1.30	L.L.	12	-1.30	L.L.	1	-2.01	0.08	-2.35	0			
GRB011211	$20.40^{+0.20}_{-0.20}$	2	-1.36	L.L.	0			11	-1.36	L.L.	2	-1.80	L.L.		0			
GRB020813	22^a	2	-1.31	L.L.	2	-1.17	L.L.	12	-1.17	L.L.	2	-2.10	L.L.	-1.94	0			
GRB030226	$20.50^{+0.30}_{-0.30}$	2	-1.31	L.L.	3	-0.47	U.L.	11	-1.31	L.L.	1	-1.05	0.18		0			
GRB030323	$21.90^{+0.07}_{-0.07}$	2	-1.56	L.L.	2	-0.87	L.L.	12	-0.87	L.L.	1	-2.40	0.43		0			
GRB050401	$22.60^{+0.30}_{-0.30}$	2	-2.16	L.L.	2	-1.57	L.L.	12	-1.57	L.L.	2	-2.30	L.L.		0			
GRB050505	$22.05^{+0.10}_{-0.10}$	-4	-1.25	L.L.	0			11	-1.25	L.L.	2	-1.35	L.L.		0			
GRB050730	$22.15^{+0.10}_{-0.10}$	4	-2.26	0.10	0			4	-2.26	0.14	1	-2.50	0.12		1	-3.16	0.10	13.2
GRB050820	$21.00^{+0.10}_{-0.10}$	4	-0.63	0.04	1	-0.71	0.02	4	-0.63	0.11	1	-1.60	0.09	-0.80	2	-1.35	L.L.	12.7
GRB050904	$21.30^{+0.20}_{-0.20}$	-4	-1.10	L.L.	0			11	-1.10	L.L.	0				0			
GRB050922C	$21.60^{+0.10}_{-0.10}$	4	-2.03	0.10	3	-2.02	U.L.	4	-2.03	0.14	1	-2.63	0.01	-1.60	3	-4.09	U.L.	12.9
GRB051111	22^a	2	-1.42	L.L.	2	-0.96	L.L.	12	-0.96	L.L.	1	-2.14	0.01	-2.23	0			13.0
GRB060206	$20.85^{+0.10}_{-0.10}$	4	-0.85	0.15	0			4	-0.85	0.18	0				0			
GRB060418	22^a	2	-1.67	L.L.	1	-1.65	0.04	2	-1.65	1.00	1	-2.24	0.03	-2.23	0			12.9

circumstellar medium which hosted the GRB. Instead, we contend the gas is associated with the nearby ISM of the galaxy. This hypothesis, however, must account for the large N_{HI} values while allowing for an evacuated volume (i.e. H II region) with radius 100 pc or more.

To explore this point further, we considered an H I disk described by a double exponential⁷,

$$n(Z, R) = \frac{N_0}{h} \exp\left(\frac{-|Z|}{h}\right) \exp\left(\frac{-R}{R_d}\right), \quad (1)$$

with scale-height h , disk length R_d , and central H I column density N_0 . We searched a wide parameter space of h/R_d , N_0 , and radius of the H II region r_{HII} . Over-plotted on Figure 2 is the prediction for random sightlines originating at the center and mid-plane ($R = Z = 0$) of an exponential disk with $\log N_0 = 22$, $h/R_d = 0.1$ and $r_{\text{HII}} = 4h$. This is a reasonably good description of the observed distribution ($P_{\text{KS}} = 11\%$); an ambient ISM characterized by $\log N_0 = 22$ with a large H II region ($r_{\text{HII}} > 2h$) produces a reasonable model for the observed N_{HI} distribution. It would be worthwhile to consider this model within the context of star forming galaxies in cosmological simulations.

The association of GRB with star-forming regions raises the possibility that a significant fraction of the gas in GRB-DLAs is molecular. Conveniently, H_2 gives rise to several band heads at $\lambda \approx 1000 \text{ \AA}$ and one can directly measure the H_2 column density. For optical spectroscopy, this requires $z_{\text{GRB}} > 2$ and blue wavelength coverage. It is also important to have relatively high resolution to disentangle the absorption lines from the $\text{Ly}\alpha$ forest. Tumlinson *et al.* (2007) have recently presented an analysis of five GRB sightlines and set an upper limit to the molecular fraction $f(\text{H}_2) < 10^{-5}$ in four of the systems. The only possible detection is along the sightline to GRB 060206 with $f(\text{H}_2) \approx 10^{-3.5}$ (Fynbo *et al.* 2006), and even this value is likely to be an upper limit (Tumlinson *et al.* 2007). Therefore, we will assume that N_{H_2} is a small fraction of the total hydrogen column density. These results lend further support to the interpretation of GRB-DLAs as being dominated by ambient ISM instead of gas local to the progenitor.

Lastly, there is the contribution to $N(\text{H})$ from H^+ . Out to distances of several 10 pc, the star formation region (or GRB afterglow) will have produced an H II region with a potentially large $N(\text{H}^+)$ value. That is, unless stellar winds from the GRB progenitor have nearly evacuated the region altogether. There is, of course, no direct means of measuring the H^+ column density. Instead, we restrict our analysis of the metal column density to the atoms and ions that are dominant in neutral regions. These are termed “low-ions” – Si^+ , Fe^+ , C^+ , O^0 . We caution that low-ions are not entirely absent from H II regions (e.g. Howk & Sembach 1999), although the expected contribution would be small compared to neutral gas for $N_{\text{HI}} > 10^{21} \text{ cm}^{-2}$. A detailed treatment of the ionization state of GRB-DLAs will be presented in a future paper. Here, we will assume that ionization corrections are small and comment on conclusions which are sensitive to this assumption.

3.2. GRB-DLA Metallicities

Ideally, the metal column density is derived from a single or set of unsaturated, resolved transitions of a low-ion. We will not attempt to measure the total column density of each element (i.e. by summing all of the ionization states of a given element) but only the state which is dominant in neutral hydrogen regions (the low-ion). This can generally be achieved from spectra with high-resolution observations and modest signal-to-noise ratio. To date, however, many GRB spectra have been acquired with low-resolution spectrometers. These observations may provide accurate measurements of the equivalent widths (EWs) of strong lines, but precise column densities are difficult to derive due to modeling the line-profile (Jenkins 1986). The high-resolution observations of GRB-DLAs, however, indicate that the metal-line profiles are comprised of multiple components (termed ‘clouds’) which exhibit a bimodal distribution of column densities (Prochaska 2006). In most cases, the total column density is dominated by a single or few clouds whereas the equivalent width is the net sum of many weak clouds (Paper II). When the cloud column densities exhibit a bimodal distribution, the single-component COG analysis systematically underestimates the ionic column densities (Jenkins 1986; Prochaska 2006). In the following, we will use low-resolution EW observations only to set lower limits to column density measurements and exclude these from relative chemical abundances.

Table 3 summarizes the abundance measurements for the GRB-DLAs. We have corrected ions which exhibit fine-structure splitting of the ground-state (e.g. Fe^+) by the observed contribution of these levels. In general, this implies an increment of $< 0.05 \text{ dex}$. In five cases the H I column density and a non-refractory or mildly refractory metal abundance have been precisely measured. For the remainder of cases, we report a lower limit to the metallicity because the metal abundance is a lower limit and/or there is no spectral coverage of the $\text{Ly}\alpha$ transition. In the latter cases, we have assumed $N_{\text{HI}} = 10^{22} \text{ cm}^{-2}$ which is approximately the mean $\log N_{\text{HI}}$ value of GRB-DLAs.

We have evaluated the metallicity of the gas by adopting (in order of preference) the $[\text{S}/\text{H}]^8$ value, the $[\text{Si}/\text{H}]$ value, the $[\text{Zn}/\text{H}]$ value, or the maximum of these if each has only a lower limit value. We prefer S and Si to Zn because these elements are $\approx 1000\times$ more abundant and because Zn has an uncertain nucleosynthetic origin (Hoffman *et al.* 1996). Again, we avoid highly refractory elements like Fe and Ni (even though they may dominate the opacity in stellar atmospheres and therefore are particularly relevant within the collapsar model) because these elements may be depleted from the gas-phase.

Figure 3 presents the metallicity measurements for the GRB-DLAs as a function of the age of the universe (set by z_{GRB}) assuming the concordance cosmology ($\Omega_{\Lambda} = 0.72$, $\Omega_m = 0.28$, $h = 0.73$; Spergel *et al.* 2006). Over-plotted on the figure are the metallicity measurements for the statistical sample (HR-S) of QSO-DLAs. We restrict the discussion in this section to $t < 3.5 \text{ Gyr}$ (i.e. $z > 1.65$) where all of the GRB-DLAs have measured N_{HI} values. It is apparent that both the GRB-DLAs and QSO-DLAs exhibit a large dispersion of values. The peak-to-peak range is $\approx 2 \text{ dex}$, much larger than observational uncertainty. Second, both samples exhibit a metallicity ‘floor’ at ap-

⁷The following results are not too sensitive to the functional form of the radial profile.

⁸ $[\text{X}/\text{Y}] = \log(X/Y) - \log(X/Y)_{\odot}$

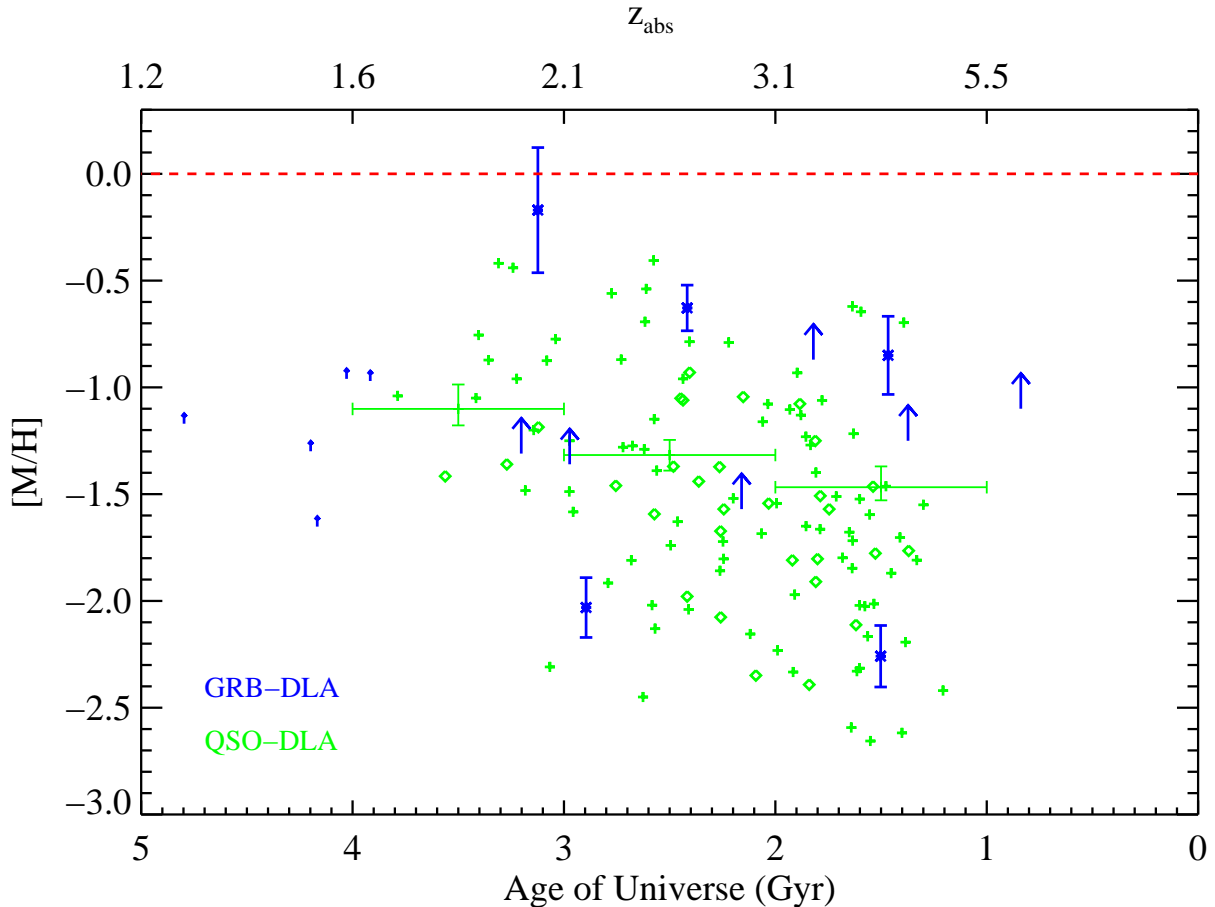


FIG. 3.— Metallicity $[M/H]$ measurements for the GRB-DLAs (dark blue) as a function of the age of the universe corresponding to the observed absorption redshift and assuming the current concordance cosmology (Spergel *et al.* 2006). At $z < 1.6$ where Ly α is lost below the atmosphere, the small arrows indicate lower limits to the metallicity assuming $N_{\text{HI}} = 10^{22} \text{ cm}^{-2}$. At $z > 1.6$, the lower limits to $[M/H]$ for the GRB-DLAs are due to line-saturation. The lighter points show measurements for the QSO-DLAs assuming the HR-S sample (Prochaska *et al.* 2003). The plus signs indicate $N_{\text{HI}} < 10^{21} \text{ cm}^{-2}$ and the diamonds correspond to $N_{\text{HI}} \geq 10^{21} \text{ cm}^{-2}$. We also present the cosmic mean metallicity derived from the QSO-DLAs by taking the H I-weighted mean of the individual data points. Comparing the two distributions, we note that the majority of GRB-DLA values lie above the cosmic mean and that a significant fraction have $[M/H] > -1$.

proximately 1/1000 solar abundance. This lower limit to the metallicities is also not observational; the sensitivity limit of the data is at least an order of magnitude lower. It remains an open question whether this floor is associated with early (PopIII) enrichment or rapid local enrichment in all galaxies exhibiting DLAs (Wasserburg & Qian 2000; Prochaska *et al.* 2003; Qian & Wasserburg 2003).

Also over-plotted in Figure 3 is the cosmic mean metallicity of atomic gas. This quantity is derived from the N_{HI} -weighted mean of QSO-DLA metallicities (Lanzetta 1993; Prochaska *et al.* 2003). Six of the 10 GRB-DLAs with N_{HI} measurements exceed the cosmic mean and several lower limits lie at the cosmic mean. Therefore, many and likely most of the GRB-DLAs have metallicities exceeding the cosmic mean in the ambient ISM of high z galaxies. On these grounds, at least, the GRB-DLAs at high z do not appear to show a significant metallicity bias toward low values.

Figure 4 presents a histogram of $[M/H]$ values for the GRB-DLAs and QSO-DLAs (restricted to $z > 1.6$). The solid bars indicate GRB-DLA values while the dark open

bars show lower limits to $[M/H]$ for the GRB-DLAs. We observe that the GRB-DLA values roughly overlap the QSO-DLA distribution. A proper treatment of the observations is to perform a two-sample survival analysis (Feigelson & Nelson 1985). Using the ASURV software package, we ran standard Gehan, logrank, and Peto-Peto tests using the Kaplan-Meier estimator and found the null hypothesis is ruled out at 99% c.l. We conclude that the metallicities of GRB-DLAs are larger than those for QSO-DLAs at $z > 1.6$.

We note that many of the GRB-DLAs have a metallicity greater than 1/10 solar. At first glance, this appears to contradict assertions that GRB progenitors have metallicity less than $0.1 Z_{\odot}$ (Langer & Norman 2006; Woosley & Heger 2006). We will demonstrate in the next section, however, that the gas-phase abundances of S, Si, and Zn are all enhanced relative to Fe. The data allow, but do not require, that the abundance of Fe is ≈ 0.5 dex lower than the $[M/H]$ values. It is possible, therefore, that at high z the GRB-DLA metallicities are not biased low and also that $[\text{Fe}/H] < -1$ in most cases. Finally, the gas that we

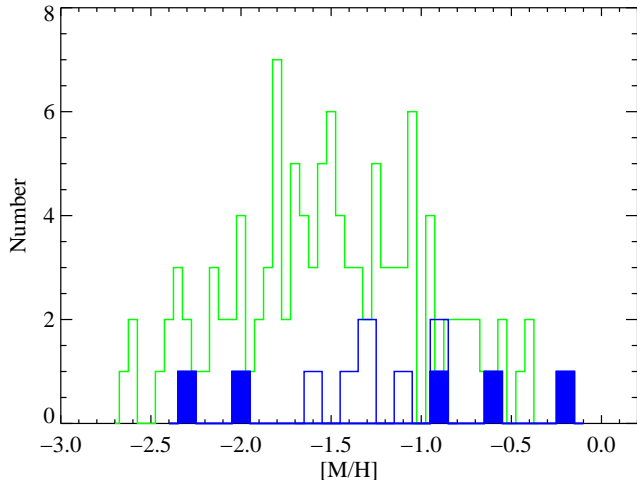


FIG. 4.— Histogram of $[M/H]$ measurements for the QSO-DLAs (light green) and the GRB-DLAs (dark) with both samples restricted to $z > 1.6$. For the GRB-DLAs, the open histogram traces the lower limits to $[M/H]$ because of line-saturation. If these values are evaluated as measurements, then the two distributions are consistent with being drawn from the same parent population. If we increment the lower limits by $+0.3$ dex, however, the null hypothesis is ruled out at $> 99\%$ c.l. by a two-sided KS test. Similarly, a two-sample survival analysis (Feigelson & Nelson 1985) rules out the null hypothesis at greater than 99% c.l.

observe is many 10 pc’s away from the progenitor and need not accurately reflect its metallicity. At present, however, we have no reason to suspect that the ISM values would systematically overestimate the GRB progenitor metallicity.

3.3. Relative Abundances

We now turn our attention to the relative abundances of the GRB-DLAs. These are measured by comparing the gas-phase column densities of pairs of low-ions (X_i , Y_i) under the assumption that ionization corrections are small, i.e. $[X/Y] = \log N_{X_i} - \log N_{Y_i} - \log(X/Y)_\odot$. With high resolution observations and moderate S/N data, one can frequently achieve 0.05 dex precision or better for $\log N_{X_i}$. Because the observed ratios represent gas-phase abundances, however, the values reflect a combination of the underlying nucleosynthetic pattern and the effects of differential depletion onto dust grains. It is unfortunate that there is no element in the Fe peak which is non-refractory. As such, observers frequently employ Zn (a neighbor of the Fe peak) as a surrogate for Fe because it is non-refractory and because it traces Fe in the Galaxy at $[Fe/H] > -2$ (Snedden, Gratton & Crocker 1991). We note, however, that Zn has an uncertain nucleosynthetic origin and should not directly trace Fe in galaxies whose star formation history differs from the Milky Way (Fenner, Prochaska & Gibson 2004). Therefore, we consider it to be a surrogate for Fe but with a large systematic uncertainty.

Throughout this section we restrict the QSO-DLA sample to the high precision echelle measurements (sample HR-E; Table 1).

3.3.1. α/Fe

A key nucleosynthetic diagnostic of stars and galaxies is the α/Fe ratio, where α refers to the sequence of He fusion in massive stars, i.e. O, Mg, Si, S, Ar. Standard theory of nucleosynthesis predicts these elements are predominantly produced by massive stars (e.g. Woosley & Weaver 1995). Therefore, a comparison of the α abundance with the Fe-peak observations, whose production is dominated by the Type Ia SN of less massive stars, constrain the age and star formation history of the galaxy when plotted against gas metallicity (Tinsley 1979). Unfortunately, O and Mg are difficult to measure via UV absorption lines because the transitions are either too strong or too weak. Instead, one typically estimates the α abundance with Si or S. In the QSO-DLAs, $[S/Si] \approx 0$ and the elements are roughly interchangeable (Prochaska & Wolfe 2002). For the GRB-DLAs, we have also adopted these two elements as the reference for α . The Fe-peak abundance, meanwhile, is determined from Fe, Ni, or Cr.

Figure 5a presents the observed α/Fe ratios for the GRB-DLAs against the QSO-DLAs as a function of α abundance, $[\alpha/H]$. We reemphasize that these gas-phase abundances have not been corrected for differential depletion. Consider, first, the values for the QSO-DLAs. At low metallicity ($[\alpha/H] < -1.5$), the QSO-DLAs follow a well-defined ‘plateau’ at $[\alpha/Fe] \approx 0.25$ dex (Prochaska & Wolfe 2002). This plateau matches the one observed for metal-poor Galactic stars (McWilliam 1997) suggesting the α/Fe enhancement has a nucleosynthetic origin (Lu *et al.* 1996; Dessauges-Zavadsky *et al.* 2006). At higher metallicity, the mean and dispersion of $[\alpha/Fe]$ rises, in stark contrast to the α/Fe trend in the Milky Way and that expected for other star formation histories (e.g. Smecker-Hane *et al.* 2002). The increase in α/Fe with increasing metallicity is a clear signature for differential depletion (Prochaska & Wolfe 2002), i.e., large $[\alpha/Fe]$ ratios at high metallicity result from the greater adsorption of Fe onto dust grains.

Turning to the GRB-DLAs, all of the $[\alpha/Fe]$ measurements are consistent with at least $+0.5$ dex and the majority lie at greater than $+0.6$ dex. Two-sample survival analysis tests (e.g. Gehan) report a less than 0.1% probability that the $[\alpha/Fe]$ values of the QSO-DLAs and GRB-DLAs are drawn from the same parent population. We conclude that the GRB-DLAs have systematically higher $[\alpha/Fe]$ ratios than the QSO-DLAs. The question that follows is whether these higher values indicate enhanced α abundances (nucleosynthesis) and/or a higher depletion level for Fe (dust).

From the nucleosynthetic viewpoint, one expects enhanced α/Fe in the gas near GRBs because (i) the progenitors are massive stars and (ii) the high specific star formation rates of their host galaxies imply ages that are young compared to the time-scales for Type Ia enrichment (Christensen, Hjorth & Gorosabel 2004). We contend that $[\alpha/Fe] > +0.3$ dex is strongly expected for GRB-DLA gas from nucleosynthesis enrichment alone (see also Calura, Dessauges-Zavadsky & Prochaska 2007). Regarding dust, one may expect high depletion levels for gas in or near star forming regions. This could also explain the offset in α/Fe between the GRB-DLAs and QSO-DLAs, especially if GRB-DLAs have systematically higher metallicity (§ 3.2).

In the next subsection, we will consider dust in greater

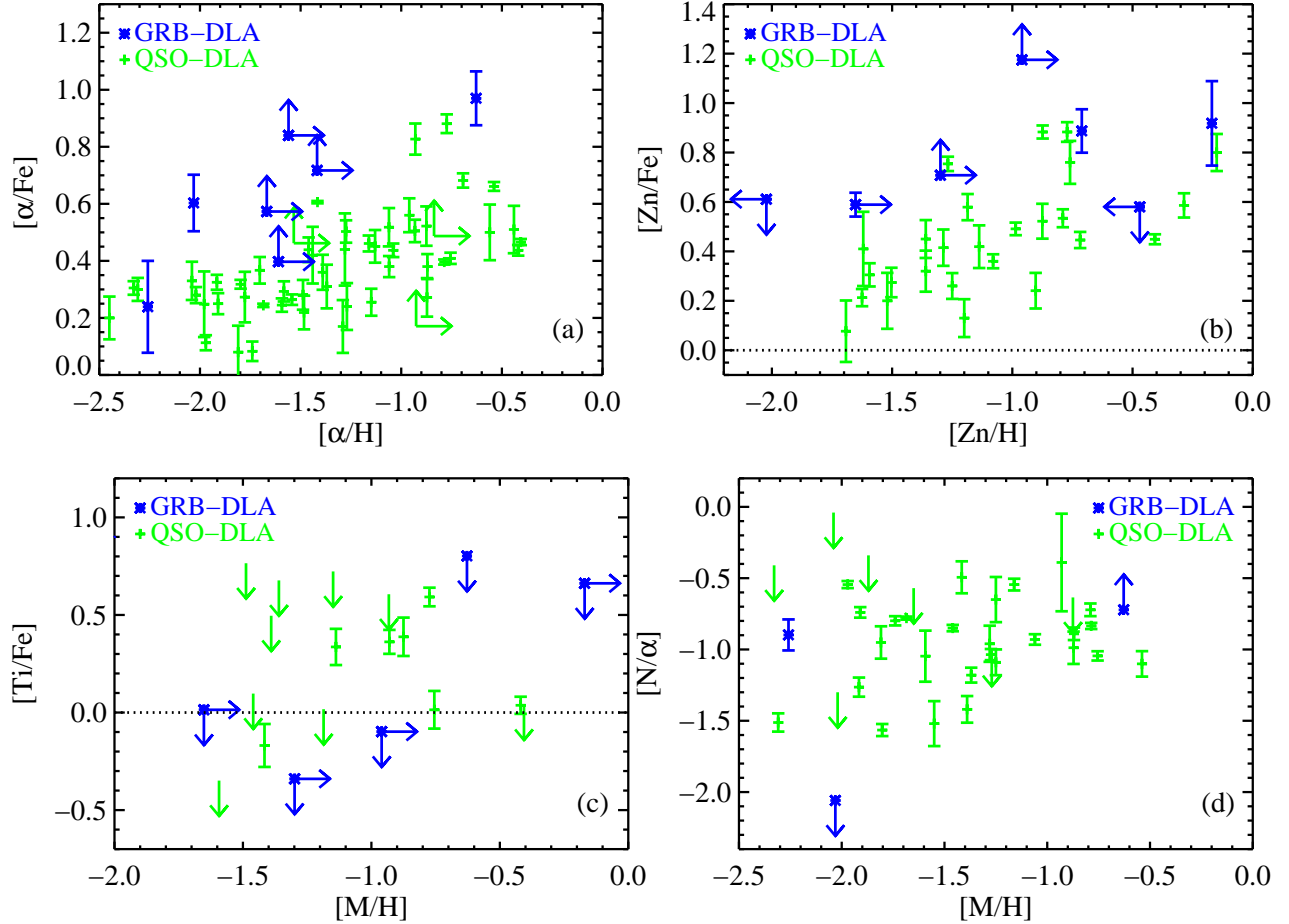


FIG. 5.— Observed gas-phase relative abundances as a function of alpha abundance $[\alpha/\text{H}]$, zinc abundance $[\text{Zn}/\text{H}]$, or metallicity $[\text{M}/\text{H}]$. The four panels show the values for GRB-DLAs and QSO-DLAs (sample HR-E) for (a) $[\alpha/\text{Fe}]$ ratios, (b) $[\text{Zn}/\text{Fe}]$ ratios, (c) $[\text{Ti}/\text{Fe}]$ ratios, and (d) $[\text{N}/\alpha]$ ratios. The GRB-DLAs are characterized by large $[\alpha/\text{Fe}]$ and $[\text{Zn}/\text{Fe}]$ ratios indicating significant nucleosynthetic enhancement by massive stars and/or differential depletion. One also notes several solar and sub-solar upper limits on $[\text{Ti}/\text{Fe}]$ which are strong evidence that refractory metals are depleted onto dust grains in GRB-DLAs.

depth. Before proceeding, we wish to emphasize the relatively low α/Fe value for GRB 050730: $[\alpha/\text{Fe}] = 0.25 \pm 0.15$ at $[\alpha/\text{H}] = -2.25$. If we were to interpret this α/Fe ratio in terms of depletion, the intrinsic (nucleosynthetic) ratio would be approximately solar or even sub-solar; this would require star-formation with low efficiency over time-scales of a few 100 Myr (Calura, Matteucci & Vladilo 2003; Dessauges-Zavadsky *et al.* 2007). This mode of star formation does not appear common for high z GRB host galaxies (Christensen, Hjorth & Gorosabel 2004). In this one case, we argue that the gas is essentially undepleted. One may speculate further that the majority of QSO-DLAs at low metallicity are also nearly undepleted and that their observed α/Fe ratios simply imply significant α -enrichment.

3.3.2. Differential Depletion

It is routine in QSO-DLA studies to examine the Zn/Fe ratio to gauge the level of differential depletion (or Zn/Cr ; Meyer & Roth 1990; Pettini *et al.* 1994). As discussed above, this assumes that the nucleosynthetic production of Zn tracks the Fe peak closely such that enhancements in the gas-phase abundance of Zn/Fe is primarily due to Fe depletion. While this assumption should be questioned at

the level of a few tenths dex (e.g. Prochaska *et al.* 2000), large Zn/Fe enhancements – especially at high metallicity – are unlikely to be explained by nucleosynthesis alone.

We present the Zn/Fe ratios of GRB-DLAs and QSO-DLAs in Figure 5b. Similar to the α/Fe ratios, the Zn/Fe values for the QSO-DLAs increase with metallicity. Again, this is best explained by higher depletion levels at higher metallicity. The GRB-DLAs do not exhibit this trend; the values are uniformly large. This suggests that the majority of GRB-DLAs have large dust-to-metal ratios. Given the uncertainty on the nucleosynthesis of Zn, however, it is best to address this issue from yet another angle.

In Figure 5c we present upper limits to the Ti/Fe ratios of those GRB-DLAs with observations of the $\text{Ti II } \lambda 1910$ transitions. In stellar atmospheres, Ti behaves like an α -element (i.e., Ti tracks Si, O, Mg in metal-poor stars; McWilliam 1997; Prochaska *et al.* 2000). In the Galactic ISM, Ti is highly refractory and one generally observes $[\text{Ti}/\text{Fe}]_{\text{ISM}} < 0$ (Jenkins 1987). Therefore, Dessauges-Zavadsky, Prochaska & Pettini (2002) emphasized that observations of Ti/Fe lend to degenerate-free interpretation: super-solar Ti/Fe ratios indicate α -enhancement whereas sub-solar Ti/Fe ratios require differential depletion. Therefore, the GRB-DLAs with $[\text{Ti}/\text{Fe}] \lesssim$

0 dex imply substantial depletion, especially in light of the large α/Fe ratios. We consider this definitive evidence that at least some GRB-DLAs are highly depleted.

The results in Figures 5b,c argue that the GRB-DLAs have at least modest depletion levels. We contend that differential depletion contributes at least +0.3 dex to $[\alpha/\text{Fe}]_g$ for most GRB-DLAs, i.e. at least 50% or more of the Fe is locked into dust grains. It remains an open question, therefore, whether the intrinsic α/Fe ratios of GRB-DLAs are enhanced relative to solar as expected for young, star-forming regions (e.g. Calura, Dessauges-Zavadsky & Prochaska 2007). While common practice is to examine the α/Zn ratio (again, using Zn as a proxy for Fe), these results are especially subject to the nucleosynthetic history of Zn. Nevertheless, examining α/Zn we find that the GRB-DLAs primarily show lower limits that are consistent with the solar abundance but allow for large enhancements. In passing, we note that a large dataset of α/Zn measurements for the GRB-DLAs could inform the processes of Zn production and also interpretations of these measurements in QSO-DLAs (Nissen *et al.* 2004).

3.3.3. N/α

Another abundance ratio of particular interest in terms of nucleosynthesis is N/α . Because N is believed to be produced primarily in the AGB phenomenon of intermediate mass stars (e.g. Meynet & Maeder 2002), the N/α ratio provides a diagnostic of the star formation history of the galaxy, especially at early times (Henry, Edmunds & Köppen 2000). Atomic nitrogen is the dominant ionization state in neutral regions and, unfortunately, this low-ion's transitions all lie within the Ly α forest. Therefore, the N abundance is difficult to measure in absorption-line systems: high resolution data is required and line-profile analysis is often required to recover N^0 column densities. Because N is non-refractory, the observed ratios should nearly correspond to the intrinsic values. The only serious systematic uncertainties are ionization corrections (Prochaska *et al.* 2002) which should be small for GRB-DLAs given the very large H I column densities.

The current GRB-DLA sample only allows one to constrain the N^0 column density for three GRB-DLAs: GRB050730, GRB050820, GRB050922C. The N/α ratios are presented in Figure 5d in comparison with measurements made for the QSO-DLAs (Prochaska *et al.* 2002; Centurión *et al.* 2003; Dessauges-Zavadsky *et al.* 2006). Although this is a small sample, it is evident that there is a large dispersion in $[N/\alpha]$ for the GRB-DLAs. This indicates that their host galaxies have experienced a diverse range of star formation histories.

Two of the N/α values (GRB 050820, GRB 050730) bracket the locus of observations for the QSO-DLAs. These values are relatively high ($[N/\alpha] \geq -1$) indicating a significant enhancement by intermediate mass stars. This is not surprising for GRB 050820 where the gas metallicity is large, implying several generations of star formation. The N/α value for GRB 050730 (at metallicity $[M/H] \approx -2$) suggests an age older than 200 Myr (Henry, Edmunds & Köppen 2000), which at $z = 4$ implies a formation redshift approaching the epoch of reionization.

The most intriguing measurement, however, is the upper limit to N/α in GRB 050922C. This limit lies well

below even the so-called lower plateau of QSO-DLA values (Prochaska *et al.* 2002; Centurión *et al.* 2003). If this upper limit has a nucleosynthetic origin, it implies gas that has not been polluted by any intermediate mass stars. Given this rather extreme value, it is important to further address ionization corrections; perhaps the low N/α value indicates an unusual ionization state for the gas (i.e. a high N^+/N^0 ratio). Because atomic nitrogen has a relatively large cross-section to X-rays (Sofia & Jenkins 1998), it may be under-abundant even in neutral regions. Both the GRB afterglow and the progenitor imply an enhanced radiation field which could lead to high N^+/N^0 ratios. We are especially concerned about photoionization for GRB 050922C given that it has a low Mg^0 column density and likely absorption by the N V doublet (Piranomonte *et al.* 2007). Equilibrium photoionization calculations, however, indicate ionization corrections are generally less than 0.5 dex, even for an input spectrum as hard as a quasar (Prochaska *et al.* 2002). In a future paper, we will perform a time-dependent calculation to track the effects of the afterglow on this and other ionization states relevant to our observations.

Unless the ionization corrections are larger than 0.5 dex, the limit on $[N/\alpha]$ lies below that of any other astrophysical environment. This is not especially surprising for a GRB event, however, especially one with very low metallicity. In this case, the galaxy may have initiated star formation only very recently and the observed metals may have no contribution from intermediate mass stars. For a standard initial mass function, this requires an enrichment age of less than ~ 30 Myr (Henry & Prochaska 2007). Future observations will reveal whether low N/α values are characteristic of a larger sample of GRB-DLAs.

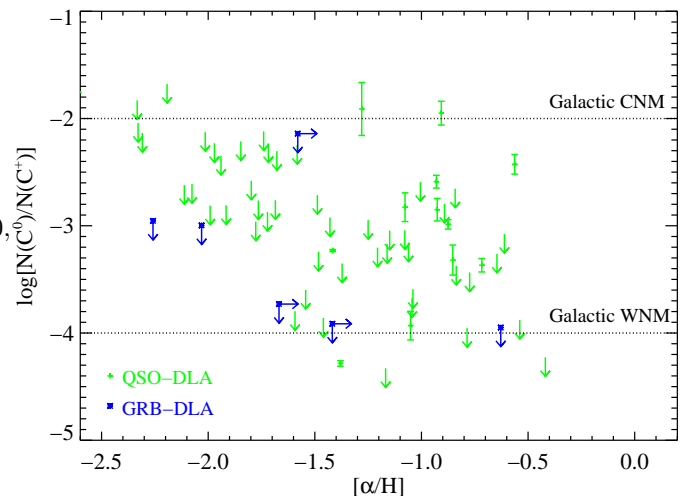


FIG. 6. — C^0/C^+ ratios of the GRB-DLAs (dark) and QSO-DLAs (light) inferred from column density measurements of C I transitions and by assuming $\log N(C^+) = [\alpha/H] + \log N_{\text{HI}} - 4$. Typical values of the cold neutral medium of the Galactic ISM are $C^0/C^+ = 10^{-2}$ (Jenkins & Shaya 1979) while significantly lower values (10^{-4}) correspond to the warm neutral medium (Liszt 2002). We interpret the observations as more reflective of the latter phase of the ISM, but caution that the results are sensitive to the far-UV intensity, metallicity, and cosmic-ray flux through the gas.

3.4. Atomic Carbon

In the Galaxy, an excellent tracer of cold, dense gas is atomic carbon. Because C^0 has an ionization potential below 1 Ryd, it is generally photoionized by the ambient far-UV radiation field of the ISM. In cold and dense regions, however, the recombination rate (proportional to the electron and carbon densities) is sufficiently large that cold clouds frequently show detectable absorption from C I transitions (e.g. Jenkins & Tripp 2001). For standard Galactic ISM conditions, the C^0/C^+ ratio is $\approx 10^{-2}$ in the cold neutral medium and decreases to $\approx 10^{-4}$ in the warm neutral medium (Liszt 2002). These ratios, of course, are sensitive to the gas metallicity, far-UV radiation field, and cosmic ray flux of the ISM (Liszt 2002; Wolfe, Prochaska & Gawiser 2003). Nevertheless, very low C^0/C^+ values generally imply gas with density less than 10 particles per cm^3 .

Figure 6 presents the C^0/C^+ ratios estimated for the GRB-DLAs and QSO-DLAs (sample HR-A). While we can measure $N(C^0)$ directly from C I transitions, the C II transitions are generally too saturated to provide even a valuable lower limit to $N(C^+)$. Therefore, we infer $N(C^+)$ from the $[\alpha/H]$ abundance and N_{HI} value, assuming $[\alpha/C]=+0.3$ (i.e. a modest α -enhancement; Akerman *et al.* 2004):

$$\log N(C^+) = [\alpha/H] + \log N_{\text{HI}} - 12 + 8.3 \quad (2)$$

Note that this calculation is actually independent of the N_{HI} value. None of the GRB-DLAs in our sample has a positive detection, although Vreeswijk *et al.* (2006) report the detection of C I in GRB-DLA 060418 with a value consistent with our upper limit. Because the metal-line column densities of the GRB-DLAs are large, the upper limits to C^0/C^+ generally lie below those of the QSO-DLAs even though the latter are derived from higher S/N data. The observations suggest the gas in GRB-DLAs (and many QSO-DLAs) is dominated by a warm, less dense phase. We caution again, however, that the predicted C^0/C^+ values are sensitive to the far-UV flux, which is likely to be enhanced near GRB. A more cautious interpretation of the data is that it offers additional, yet non-conclusive support that GRB-DLA gas is not characteristic of the Galactic cold neutral medium.

4. DISCUSSION

4.1. General Characteristics of the ISM Near Star Forming Regions

Reviewing the results presented in the previous section, we summarize the properties of gas observed surrounding GRB afterglows as having:

- Very large H I column densities with median $N_{\text{HI}} \approx 10^{21.6} \text{ cm}^{-2}$.
- A wide range of metallicities (1/100 to nearly solar) with median larger than 1/10 solar.
- Observed α/Fe ratios in excess of $3\times$ the solar abundance reflecting enrichment by massive stars (Type II SN) and/or differential depletion.

- Large $[\text{Zn}/\text{Fe}]$ values and several solar or sub-solar $[\text{Ti}/\text{Fe}]$ upper limits which indicate substantial differential depletion.
- A dispersion of $[\text{N}/\alpha]$ indicating a diverse set of star formation histories. We identify one case (GRB 050922C) with an extremely low value suggesting gas enriched solely by massive stars.

At first glance, the observation of large H I surface densities and significantly depleted, chemically enriched gas appear to reflect the conditions expected for actively star-forming regions (i.e. molecular clouds). Quantitatively, however, we find that the GRB-DLA properties are more characteristic of the ambient ISM of modern galaxies. As several authors have noted for individual GRB-DLA (Savaglio & Fall 2004; Penprase *et al.* 2006; Shin *et al.* 2006), the observed depletion levels are more representative of warm (i.e. less dense) clouds in the Galactic ISM (see also Savaglio 2006). On the other hand, the majority of GRB-DLAs have sub-solar metallicity and a direct comparison with the Galactic ISM may not be appropriate. Unfortunately, the differential depletion characteristics of cold, dense gas in other galaxies (e.g. the Magellanic clouds) has not been extensively measured, in part because dust obscuration challenges the analysis. In the Small Magellanic Cloud (SMC), one does observe highly depleted gas along the sightline to Sk 155 but one also finds modest depletions in clouds where C I analysis indicates large density ($> 100 \text{ cm}^{-3}$ Welty *et al.* 2001; Sofia *et al.* 2006; Welty *et al.* 2006). We cautiously conclude that the depletion levels observed for the GRB-DLAs are generally lower than that observed for cold, dense clouds in the local universe. It would be very valuable to independently estimate the density of gas responsible for GRB-DLAs.

Throughout this paper, we have presented additional observations which argue the GRB-DLAs do not arise in a cold, dense phase. First, the gas has very low molecular fraction (Vreeswijk *et al.* 2004, Paper III). Although a low molecular fraction could result from photoionization by the progenitor, nearby O and B stars, and the GRB afterglow, we have argued the gas lies at $\gtrsim 100 \text{ pc}$ from the GRB where these effects may be lessened. If the gas has large particle density ($n_H > 10^3 \text{ cm}^{-3}$), then it would be difficult to maintain such a low H_2 fraction (Paper III).

Second, the only atomic line routinely measured in the GRB-DLAs is Mg I and its large dielectronic recombination coefficient does not require cold, dense gas. In § 3.4 we presented upper limits on C^0/C^+ which argue against gas with characteristics like the dense CNM of the Milky Way. Third, there are no especially anomalous abundance patterns observed for the gas (e.g. extreme metallicity, very high α/Fe ratios) which could occur if the gas represented partially mixed SN ejecta or circumstellar material. Altogether, we conclude that the gas revealed by GRB afterglow spectra represents the ISM near the GRB but not gas directly associated with its own molecular cloud.

4.2. Comparisons with QSO-DLAs

In the previous subsection, we argued that the GRB-DLAs represent gas from the ambient ISM of their host galaxies. The large N_{HI} values of QSO-DLAs argue these

sightlines also penetrate the ISM of high z galaxies. Furthermore, the majority of QSO-DLAs have depletion patterns, low C^+0/C^+ ratios, and low molecular fractions which are not characteristic of cold, dense gas in the Galaxy. In this respect, it is fair to compare the observations of the two populations to address whether they are drawn from the same parent population of galaxies. In § 3 we compared the N_{HI} values, metallicity, and relative abundance ratios of the QSO-DLAs and GRB-DLAs. The latter are characterized by higher N_{HI} values, higher α/Fe and Zn/Fe ratios, and higher metallicities. These differences beg the question: *Are GRB-DLAs and QSO-DLAs drawn from distinct distributions of host galaxies?*

We contend that the observations presented in this paper do not contradict the null hypothesis that GRB-DLAs and QSO-DLAs have identical parent populations of galaxies but their differences can be explained by sightlines with distinct impact parameter distributions. Although offsets exist in $[\text{M}/\text{H}]$ and the X/Fe ratios, the differences are relatively small (< 0.5 dex). Typical observed gradients in the metallicity of stars and H II regions of local galaxies imply a variation of at least 0.3 dex from the center of the galaxy to the radii roughly corresponding to $N_{\text{HI}} = 2 \times 10^{20} \text{ cm}^{-2}$ (e.g. Kennicutt, Bresolin & Garnett 2003; Chen, Kennicutt & Rauch 2005; Luck, Kovtyukh & Andrievsky 2006). Furthermore, the H I surface density and volume density are undoubtedly larger toward the center of the galaxy (at least until the gas becomes molecular). And it is reasonable to expect that higher metallicity, denser gas will exhibit larger depletion levels than more tenuous gas at the outer edges of H I disks.

At present, the only distribution with an especially large offset (> 1 dex difference in median value) is the N_{HI} values. While differences in the impact parameters of GRB-DLAs and QSO-DLAs may explain the offsets in the median of the distributions for N_{HI} , $[\text{M}/\text{H}]$, and X/Fe ratios, the identification of many GRB-DLAs with $N_{\text{HI}} > 10^{22} \text{ cm}^{-2}$ and *none* in the QSO-DLA sample is striking. In § 3.1, we demonstrated that the GRB-DLA N_{HI} distribution is reasonably well explained by an H II region embedded with an exponential H I disk with central column density $\log N_0 = 10^{22} \text{ cm}^{-2}$. While this simplistic model is a good description of the observations, it does lead to a conflict with the H I frequency distribution $f(N_{\text{HI}})$ observed for the QSO-DLAs. If the majority of high z galaxies have $\log N_0 = 10^{22} \text{ cm}^{-2}$, then one would not observe a break in $f(N_{\text{HI}})$ at $N_{\text{HI}} \approx 10^{21.5} \text{ cm}^{-2}$ as observed (Prochaska, Herbert-Fort & Wolfe 2005). One possible resolution for this conflict is that GRB-DLA sightlines are obscured by dust from magnitude-limited QSO surveys. Let us now consider this hypothesis in greater detail.

4.3. Can QSO-DLA Samples Probe GRB-DLA Sightlines?

As Figure 2 reveals, a significant fraction of GRB-DLAs have $N_{\text{HI}} \geq 10^{22} \text{ cm}^{-2}$ yet not one of the ≈ 500 QSO-DLAs discovered thus far have $N_{\text{HI}} > 10^{21.9} \text{ cm}^{-2}$. An analysis of the SDSS dataset actually requires that the QSO-DLAs exhibit a break in their H I frequency distribution $f(N_{\text{HI}})$ at $N_{\text{HI}} \approx 10^{21.5} \text{ cm}^{-2}$ to explain the absence of large N_{HI} absorbers (Prochaska, Herbert-Fort & Wolfe

2005). This is most easily seen by extrapolating the $f(N_{\text{HI}}) \propto N_{\text{HI}}^{-2}$ power-law observed at $N_{\text{HI}} < 10^{21} \text{ cm}^{-2}$ to larger column densities. One predicts that there should be ≈ 10 damped Ly α systems with $N_{\text{HI}} \geq 10^{22} \text{ cm}^{-2}$ per 500 observed. The absence of a single QSO-DLA with this column density indicates that $f(N_{\text{HI}})$ has a steeper than N_{HI}^{-2} dependence at these column densities. The observation of a break in $f(N_{\text{HI}})$ and the routine observation of $N_{\text{HI}} > 10^{22} \text{ cm}^{-2}$ in GRB-DLAs raises concerns that dust obscuration is biasing the QSO-DLA sample against large N_{HI} values.

There is additional (circumstantial) evidence for a dust obscuration bias in QSO-DLAs. First, QSO-DLAs with a combination of large N_{HI} and high metallicity (metal-strong DLA), i.e. potentially large dust columns, are rare (Boisse *et al.* 1998; Herbert-Fort *et al.* 2006). Second, every DLA is enriched by heavy metals with metallicity $[\text{M}/\text{H}] > -3$ (Prochaska *et al.* 2003) and many have relative abundance ratios (e.g. Zn/Fe) indicative of differential dust depletion (Pettini *et al.* 1994; Prochaska & Wolfe 2002). Third, several quasars with intervening DLA show significant reddening that can be attributed to the absorber Vladilo *et al.* (2006). Motivated by these observations, we will test whether QSO-DLA samples would be likely to include GRB-DLA sightlines if background quasars were placed directly on the sightline.

We begin by deriving the dust-to-gas ratios of the GRB-DLAs. In the following, we will assume the GRB-DLA dust properties are best matched by those observed for the SMC. We make this choice because (i) no GRB-DLA to date has exhibited the 2175Å dust feature characteristic of the Milky Way and LMC extinction laws (e.g. Mirabal *et al.* 2002; Savaglio & Fall 2004; Ellison *et al.* 2006; Butler *et al.* 2007); and (ii) the metallicities of GRB-DLAs are representative of the SMC. We derive the dust-to-gas ratio of the DLAs relative to the SMC: $\kappa/\kappa_{\text{SMC}}$ by assuming the SMC has metallicity $[\text{M}/\text{H}]_{\text{SMC}} = -0.7$ and that 90% of its refractory elements are depleted from the gas-phase, i.e. $[\text{M}/\text{Fe}]_{\text{SMC}} = +1$ (Welty *et al.* 1997, 2001). In this case, the relative dust-to-gas ratio is

$$\frac{\kappa}{\kappa_{\text{SMC}}} = 10^{[\text{M}/\text{H}] + 0.7} \left[\frac{1 - 10^{(\Delta_i - [\text{M}/\text{Fe}])}}{1 - 10^{-1}} \right] \quad (3)$$

where Δ_i allows for a nucleosynthetic contribution to the observed $[\text{M}/\text{Fe}]$ value and we assume $\Delta_i = 0$ for the SMC. For the GRB-DLAs, we adopt the $[\text{M}/\text{H}]$ and $[\text{M}/\text{Fe}]$ values listed in Table 3. In the majority of cases, M is sulfur and the remainder assume Zn or Si. In the following, we will assume $\Delta_i = 0.3$ dex for the GRB-DLAs and 0.2 dex for the QSO-DLAs. The high specific star formation rates observed for GRB host galaxies indicate young ages and, therefore, gas enriched by massive stars giving α -enriched abundances ($[\alpha/\text{Fe}] > +0.2$). Similarly, the QSO-DLAs show a plateau of $[\text{Si}/\text{Fe}] = +0.25$ dex values at low metallicity indicative of Type II enrichment (Prochaska & Wolfe 2002), and enhanced α/Fe ratios in “dust free” systems (Dessauges-Zavadsky *et al.* 2006). In any case, the results are not sensitive to our choices for Δ_i unless we allow $\Delta_i > 0.5$ dex for the GRB-DLAs or $\Delta_i > 0.3$ dex for the QSO-DLAs.

Figure 7 shows the $\kappa/\kappa_{\text{SMC}}$ values for the GRB-DLAs and also the echelle sample (HR-E) of QSO-DLAs. Both samples exhibit a wide range of dust-to-gas ratios relative

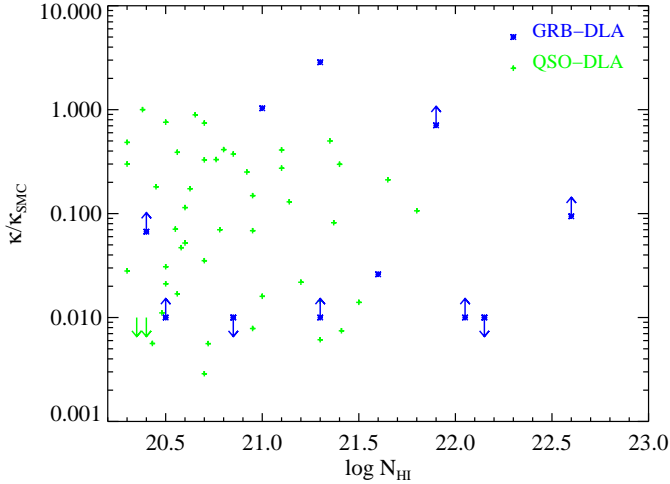


FIG. 7.— Dust-to-gas ratio κ of the GRB-DLAs (dark blue) and QSO-DLAs (light green) relative to the dust-to-gas ratio of the SMC (κ_{SMC}) as a function of H I column density.

to the SMC. We also find that the GRB-DLAs show a higher fraction of large values ($\kappa/\kappa_{SMC} \gtrsim 1$). Using the observed N_{HI} values and assuming SMC dust properties, we can convert these dust-to-gas ratios into visual extinction, A_V . Specifically, we adopt two empirical relations: (i) the observed reddening in the SMC (Tumlinson *et al.* 2002)

$$\log E(B - V) = \log N_{HI} - 22.95 \quad (4)$$

and (ii) a linear relation between A_V and $E(B - V)$ (Gordon *et al.* 2003) modified by the dust-to-gas ratio

$$A_V = 2.74 E(B - V) \frac{\kappa}{\kappa_{SMC}}. \quad (5)$$

Figure 8 presents the A_V values against H I column density for the GRB-DLAs compared against QSO-DLAs. All of the QSO-DLAs have $A_V < 0.05$ mag (see also Prochaska & Wolfe 2002). It is not surprising, therefore, that one observes very little reddening of quasar spectra by QSO-DLAs (Murphy & Chaffin 2004). In contrast, the estimated A_V values for approximately half the GRB-DLAs are substantially larger than the QSO-DLA distribution ($A_V > 0.1$ mag). At $A_V = 0.1$ mag, the extinction at the $Ly\alpha$ transition is $A_{Ly\alpha} = 0.6$ mag assuming the SMC extinction law (Prevot *et al.* 1984). This is a considerable but not overwhelming level of extinction. Interestingly, there is no obvious correlation between A_V and N_{HI} , at least for A_V values greater than 0.05 mag. We also note that the A_V values presented in Figure 8 are roughly consistent with the A_V values inferred from broad-band photometry or spectrophotometry of GRB afterglows (e.g. Mirabal *et al.* 2002; Vreeswijk *et al.* 2004; Savaglio & Fall 2004; Butler *et al.* 2006). On the other hand, our A_V values appear to be at odds with those inferred from X-ray absorption measurements (e.g. Watson *et al.* 2006; Butler *et al.* 2006) which has led some authors to invoke “grey” extinction laws for the dust enveloping GRBs (Galama & Wijers 2001). This issue will be addressed in greater detail in a future paper (Butler *et al.* 2007, in prep).

Finally, we examine whether the inferred A_V values for the GRB-DLA sightlines are sufficiently large to bias

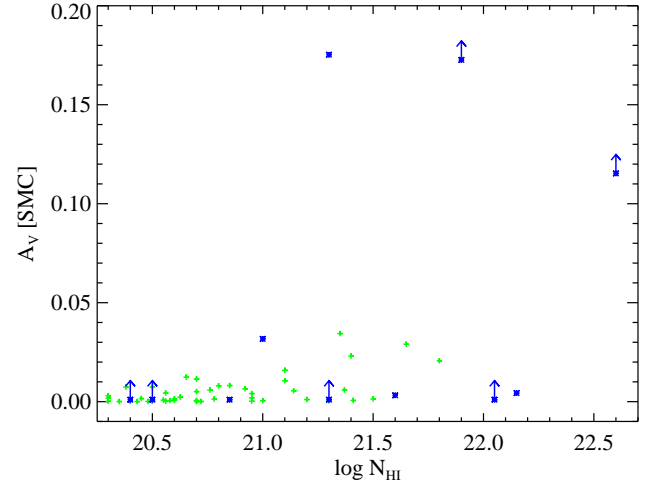


FIG. 8.— Predicted visual extinctions A_V for the GRB-DLA and QSO-DLA sightlines assuming the dust-to-gas ratios presented in Figure 7 and assuming the dust properties of the SMC (Tumlinson *et al.* 2002; Gordon *et al.* 2003). All of the QSO-DLA sightlines show very small values ($A_V < 0.05$ mag). In contrast, the GRB-DLA show a nearly bimodal population with several small values and several sightlines approaching 0.2 mag. Note that $A_V = 0.1$ mag corresponds to an extinction of 0.6 mag assuming the SMC extinction law.

against their detection in QSO samples. To estimate the effects, we assessed the signal-to-noise ratio (S/N) at the center of the $Ly\alpha$ profile of each QSO-DLAs in the SDSS-DR3 sample. Specifically, we measured the median S/N using the continuum adopted in the fits to the $Ly\alpha$ profiles by Prochaska, Herbert-Fort & Wolfe (2005). By the definition of their statistical sample, the S/N exceeds 4 pix^{-1} in each case. We then lowered the S/N by adopting an extinction A_V assuming that the noise is quasar dominated,

$$S/N = (S/N_0) / \sqrt{10^{A_{Ly\alpha}/2.5}} \quad (6)$$

The fraction of QSO-DLAs that satisfy the $S/N > 4 \text{ pix}^{-1}$ criterion is shown in Figure 9 as a function of A_V . For $A_V < 0.2$ mag, dust obscuration has a relatively small impact on the QSO-DLA sample. We cautiously conclude, therefore, that the majority of observed GRB-DLAs would also be observed along quasar sightlines.

This conclusion, however, is subject to a few caveats. First, the exercise described by Figure 9 does not account for quasars that would become too red or too faint to satisfy the QSO target criteria for the SDSS (Richards *et al.* 2004). We suspect, however, that this effect is much smaller than the S/N cut we have applied (Murphy *et al.* 2007, in prep). Second, several of the κ/κ_{SMC} values for the GRB-DLAs are lower limits because of line saturation. It is possible that these have $A_V > 0.4$ mag and would have a small probability of entering the QSO-DLA sample. Third, all of the results assume SMC extinction. This assumption has two implications: (i) it establishes the reddening per H I atom (scaled by metallicity; Equation 4) and (ii) the shape of the extinction law which determines $A_{Ly\alpha}/A_V$. Regarding the latter aspect, the SMC has the steepest extinction law of local galaxies. Other (“grayer”) dust laws would generally lead to less extinction at $Ly\alpha$. The reddening per H I atom in the SMC, however, is smaller than

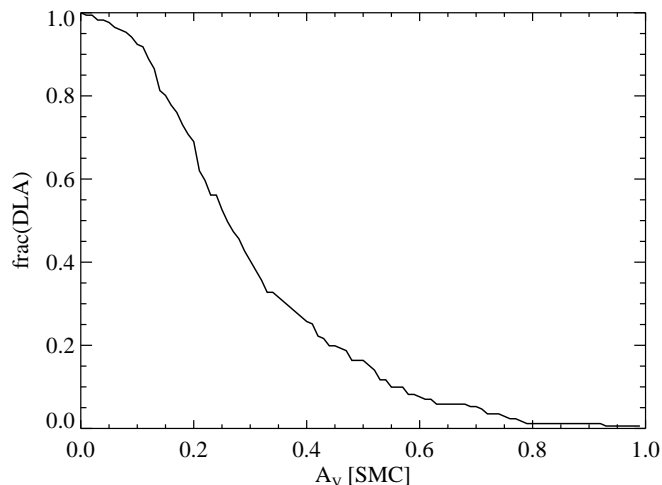


FIG. 9.— Fraction of DLAs recovered from the SDSS QSO-DLA survey of Prochaska, Herbert-Fort & Wolfe (2005) as a function of additional visual extinction (A_V) for the DLAs. For $A_V < 0.2$ mag, the effect of obscuration is mild while only a small fraction of QSO-DLAs with $A_V > 0.4$ mag would be recovered in the SDSS survey.

the Milky Way and not only because of the SMC's lower metallicity (Welty *et al.* 2006). Fourth, we have ignored the possibility that a significant column of dust exists in the H II region surrounding the GRB. This could be revealed by broad-band photometry of the afterglow compared against A_V estimations from the observed metal column densities. Finally, we note that a non-negligible fraction of GRB afterglows are severely reddened, most likely by dust surrounding the event (Levan *et al.* 2006; Pellizza *et al.* 2006). These “dark bursts” do not enter our GRB-DLA sample and likely have A_V values much larger than those presented in Figure 8. At present, this extremely dusty gas is not well probed by GRB or QSO observations.

These concerns aside, our analysis suggests that many (if not all) of the GRB-DLAs in our sample could be detected in modern QSO-DLA surveys. If confirmed by larger samples, then the very low incidence of QSO-DLAs with $N_{\text{HI}} \geq 10^{22} \text{ cm}^{-2}$ must be explained by a substantial decrease in the cross-section of gas with these column densities. To avoid conflict with the observed $f(N_{\text{HI}})$ distribution, one requires that the cross-section of the regions probed by GRB-DLAs must be less than 1% of the cross-section corresponding to the damped Ly α criterion, $\log N_{\text{HI}} = 20.3$. Characterizing the latter by a radius $r_{20.3}$, we require the $r_{\text{GRB}} < r_{20.3}/10$. This relation is rather easily achieved if r_{GRB} is 100pc or less, but could pose a problem if $r_{\text{GRB}} \gtrsim 1$ kpc (Vreeswijk *et al.* 2006).

We wish to thank Arthur M. Wolfe for helpful discussions and for allowing us to analyze results on QSO-DLAs prior to the public release of these data. We thank E. Ramirez-Ruiz for constructive comments on an early version of this manuscript. J.X.P. is partially supported by NASA/Swift grant NNG05GF55G and an NSF CAREER grant (AST-0548180).

REFERENCES

- Akerman, C. J. *et al.* 2004, *A&A*, 414, 931.
 Barth, A. J. *et al.* 2003, *ApJ (Letters)*, 584, L47.
 Berger, E. *et al.* 2006, *ApJ*, 642, 979.
 Blitz, L. 1993, in *Protostars and Planets III*, ed. E. H. Levy and J. I. Lunine, 125.
 Blitz, L. *et al.* 2007, in *Protostars and Planets V*, ed. B. Reipurth, D. Jewitt, and K. Keil, 81.
 Bloom, J. S., Kulkarni, S. R., and Djorgovski, S. G. 2002, *AJ*, 123, 1111.
 Boisse, P. *et al.* 1998, *A&A*, 333, 841.
 Butler, N. *et al.* 2007, In prep.
 Butler, N. R. *et al.* 2006, *ApJ*, 652, 1390.
 Calura, F., Dessauges-Zavadsky, M., and Prochaska, J. 2007, In prep.
 Calura, F., Matteucci, F., and Vladilo, G. 2003, *MNRAS*, 340, 59.
 Castro, S. *et al.* 2003, *ApJ*, 586, 128.
 Centurión, M. *et al.* 2003, *A&A*, 403, 55.
 Chen, H.-W., Kennicutt, Jr., R. C., and Rauch, M. 2005, *ApJ*, 620, 703.
 Chen, H.-W. *et al.* 2007, *ArXiv Astrophysics e-prints*.
 Chen, H.-W. *et al.* 2005, *ApJ*, 634, L25.
 Christensen, L., Hjorth, J., and Gorosabel, J. 2004, *A&A*, 425, 913.
 Dekker, H. *et al.* 2000, in *Proc. SPIE Vol. 4008*, p. 534-545, *Optical and IR Telescope Instrumentation and Detectors*, Masanori Iye; Alan F. Moorwood; Eds., ed. M. Iye and A. F. Moorwood, 534.
 Dessauges-Zavadsky, M. *et al.* 2007, *A&A*.
 Dessauges-Zavadsky, M. *et al.* 2006a, *ApJ*, 648, L89.
 Dessauges-Zavadsky, M. *et al.* 2001, *A&A*, 370, 426.
 Dessauges-Zavadsky, M., Prochaska, J. X., and D’Odorico, S. 2002, *A&A*, 391, 801.
 Dessauges-Zavadsky, M. *et al.* 2006b, *A&A*, 445, 93.
 Draine, B. T. and Hao, L. 2002, *ApJ*, 569, 780.
 Ellison, S. L. *et al.* 2006, *MNRAS*, 372, L38.
 Fall, S. M. and Pei, Y. C. 1993, *ApJ*, 402, 479.
 Feigelson, E. D. and Nelson, P. I. 1985, *ApJ*, 293, 192.
 Fenner, Y., Prochaska, J. X., and Gibson, B. K. 2004, *ApJ*, 606, 116.
 Fiore, F. *et al.* 2005, *ApJ*, 624, 853.
 Fruchter, A., Krolik, J. H., and Rhoads, J. E. 2001, *ApJ*, 563, 597.
 Fruchter, A. S. *et al.* 2006, *Nature*, 441, 463.
 Fynbo, J. P. U. *et al.* 2006a, *A&A*, 451, L47.
 Fynbo, J. P. U. *et al.* 2006b, *Nature*, 444, 1047.
 Galama, T. J. and Wijers, R. A. M. J. 2001, *ApJ (Letters)*, 549, L209.
 Gehrels, N. A. 2000, in *Proc. SPIE X-Ray and Gamma-Ray Instrumentation for Astronomy XI*, ed. Kathryn A. Flanagan and Oswald H. Siegmund, volume 4140, 42.
 Gordon, K. D. *et al.* 2003, *ApJ*, 594, 279.
 Guetta, D. and Piran, T. 2007, *ArXiv Astrophysics e-prints*.
 Hammer, F. *et al.* 2006, *A&A*, 454, 103.
 Henry, D. and Prochaska, J. 2007, In prep.
 Henry, R. B. C., Edmunds, M. G., and Köppen, J. 2000, *ApJ*, 541, 660.
 Herbert-Fort, S. *et al.* 2006, *PASP*, 118, 1077.
 Hjorth, J. *et al.* 2003, *Nature*, 423, 847.
 Hoffman, R. D. *et al.* 1996, *ApJ*, 460, 478.
 Howk, J. C. and Sembach, K. R. 1999, *ApJ*, 523, L141.
 Jakobsson, P. *et al.* 2006a, *A&A*, 460, L13.
 Jakobsson, P. *et al.* 2006b, *A&A*, 447, 897.
 Jenkins, E. B. 1986, *ApJ*, 304, 739.
 Jenkins, E. B. 1987, in *ASSL Vol. 134: Interstellar Processes*, ed. D. J. Hollenbach and H. A. Thronson, Jr., 533.
 Jenkins, E. B. and Shaya, E. J. 1979, *ApJ*, 231, 55.
 Jenkins, E. B. and Tripp, T. M. 2001, *ApJS*, 137, 297.
 Kawai, N. *et al.* 2006, *Nature*, 440, 184.
 Kennicutt, Jr., R. C., Bresolin, F., and Garnett, D. R. 2003, *ApJ*, 591, 801.
 Kewley, L. J. *et al.* 2007, *AJ*, 133, 882.
 Kobulnicky, H. A. and Kewley, L. J. 2004, *ApJ*, 617, 240.
 Langer, N. and Norman, C. A. 2006, *ApJ*, 638, L63.
 Lanzetta, K. M. 1993, in *ASSL Vol. 188: The Environment and Evolution of Galaxies*, ed. J. M. Shull and H. A. Thronson, 237.
 Le Floc’h, E. *et al.* 2003, *A&A*, 400, 499.
 Ledoux, C. *et al.* 2006, *A&A*, 457, 71.
 Ledoux, C., Petitjean, P., and Srianand, R. 2003, *MNRAS*, 346, 209.
 Levan, A. *et al.* 2006, *ApJ*, 647, 471.
 Liszt, H. 2002, *A&A*, 389, 393.
 Lu, L. *et al.* 1996, *ApJS*, 107, 475.
 Luck, R. E., Kovtyukh, V. V., and Andrievsky, S. M. 2006, *AJ*, 132, 902.
 McWilliam, A. 1997, *ARA&A*, 35, 503.
 Metzger, M. R. *et al.* 1997, *Nature*, 387, 879.
 Meyer, D. M. and Roth, K. C. 1990, *ApJ*, 363, 57.
 Meynet, G. and Maeder, A. 2002, *A&A*, 381, L25.

- Mirabal, N. *et al.* 2006, ApJ, 643, L99.
- Mirabal, N. *et al.* 2002, ApJ, 578, 818.
- Mo, H. J., Mao, S., and White, S. D. M. 1998, MNRAS, 295, 319.
- Modjaz, M. *et al.* 2007, ArXiv Astrophysics e-prints.
- Molaro, P. *et al.* 2001, ApJ, 549, 90.
- Murphy, M. T. and Liske, J. 2004, MNRAS, 354, L31.
- Nissen, P. E. *et al.* 2004, A&A, 415, 993.
- Pellizza, L. J. *et al.* 2006, A&A, 459, L5.
- Penprase, B. E. *et al.* 2006, ApJ, 646, 358.
- Perna, R. and Lazzati, D. 2002, ApJ, 580, 261.
- Pettini, M. *et al.* 1994, ApJ, 426, 79.
- Piranomonte, S. *et al.* 2007, A&A.
- Prevot, M. L. *et al.* 1984, A&A, 132, 389.
- Prochaska, J. *et al.* 2007a, In prep.
- Prochaska, J. X. 2006, ApJ, 650, 272.
- Prochaska, J. X. *et al.* 2004, ApJ, 611, 200.
- Prochaska, J. X. *et al.* 2006, ArXiv Astrophysics e-prints.
- Prochaska, J. X., Chen, H.-W., and Bloom, J. S. 2006, ApJ, 648, 95.
- Prochaska, J. X. *et al.* 2005, GRB Coordinates Network, 3971, 1.
- Prochaska, J. X. *et al.* 2003a, ApJ, 595, L9.
- Prochaska, J. X. *et al.* 2003b, ApJS, 147, 227.
- Prochaska, J. X. *et al.* 2002a, PASP, 114, 933.
- Prochaska, J. X. and Herbert-Fort, S. 2004, PASP, 116, 622.
- Prochaska, J. X., Herbert-Fort, S., and Wolfe, A. M. 2005, ApJ, 635, 123.
- Prochaska, J. X. *et al.* 2002b, ApJ, 571, 693.
- Prochaska, J. X. *et al.* 2000, AJ, 120, 2513.
- Prochaska, J. X. and Wolfe, A. M. 1999, ApJS, 121, 369.
- Prochaska, J. X. and Wolfe, A. M. 2002, ApJ, 566, 68.
- Prochaska, J. X. *et al.* 2007b, ArXiv Astrophysics e-prints.
- Prochaska, J. X. *et al.* 2001, ApJS, 137, 21.
- Prochter, G. E. *et al.* 2006, ApJ, 648, L93.
- Qian, Y.-Z. and Wasserburg, G. J. 2003, ApJ, 596, L9.
- Ramirez-Ruiz, E., Trentham, N., and Blain, A. W. 2002, MNRAS, 329, 465.
- Razoumov, A. O. *et al.* 2006, ApJ, 645, 55.
- Reichart, D. E. and Price, P. A. 2002, ApJ, 565, 174.
- Richards, G. T. *et al.* 2004, ApJS, 155, 257.
- Savaglio, S. 2006, New Journal of Physics, 8, 195.
- Savaglio, S. and Fall, S. M. 2004, ApJ, 614, 293.
- Savaglio, S., Fall, S. M., and Fiore, F. 2003, ApJ, 585, 638.
- Sheinis, A. I. *et al.* 2000, in Proc. SPIE Vol. 4008, p. 522-533, Optical and IR Telescope Instrumentation and Detectors, Masanori Iye; Alan F. Moorwood; Eds., 522.
- Shin, M.-S. *et al.* 2006, ArXiv Astrophysics e-prints.
- Smecker-Hane, T. A. *et al.* 2002, ApJ, 566, 239.
- Snedden, C., Gratton, R. G., and Crocker, D. A. 1991, A&A, 246, 354.
- Sofia, U. J. *et al.* 2006, ApJ, 636, 753.
- Sofia, U. J. and Jenkins, E. B. 1998, ApJ, 499, 951.
- Sollerman, J. *et al.* 2005, New Astronomy, 11, 103.
- Solomon, P. M. and Rivolo, A. R. 1989, ApJ, 339, 919.
- Spergel, D. N. *et al.* 2006, ArXiv Astrophysics e-prints.
- Stanek, K. Z. *et al.* 2006, Acta Astronomica, 56, 333.
- Stanek, K. Z. *et al.* 2003, ApJ (*Letters*), 591, L17.
- Tinsley, B. M. 1979, ApJ, 229, 1046.
- Totani, T. 1999, ApJ, 511, 41.
- Tumlinson, J. *et al.* 2007, In prep.
- Tumlinson, J. *et al.* 2002, ApJ, 566, 857.
- Vink, J. S. and de Koter, A. 2005, A&A, 442, 587.
- Vladilo, G. *et al.* 2006, A&A, 454, 151.
- Vogt, S. S. *et al.* 1994, in Proc. SPIE Instrumentation in Astronomy VIII, David L. Crawford; Eric R. Craine; Eds., Volume 2198, p. 362, 362.
- Vreeswijk, P. M. *et al.* 2004, A&A, 419, 927.
- Vreeswijk, P. M. *et al.* 2006a, ArXiv Astrophysics e-prints.
- Vreeswijk, P. M. *et al.* 2006b, A&A, 447, 145.
- Wasserburg, G. J. and Qian, Y.-Z. 2000, ApJ, 538, L99.
- Watson, D. *et al.* 2006, ApJ, 652, 1011.
- Waxman, E. and Draine, B. T. 2000, ApJ, 537, 796.
- Welty, D. E. *et al.* 2006, ApJS, 165, 138.
- Welty, D. E. *et al.* 1997, ApJ, 489, 672.
- Welty, D. E. *et al.* 2001, ApJ, 554, L75.
- White, G. J. *et al.* 1999, A&A, 342, 233.
- Wolf, C. and Podsiadlowski, P. 2006, ArXiv Astrophysics e-prints.
- Wolfe, A. M., Gawiser, E., and Prochaska, J. X. 2005, ARA&A, 43, 861.
- Wolfe, A. M., Prochaska, J. X., and Gawiser, E. 2003, ApJ, 593, 215.
- Wolfe, A. M. *et al.* 1986, ApJS, 61, 249.
- Woosley, S. E. 1993, ApJ, 405, 273.
- Woosley, S. E. 1993, ApJ, 405, 273.
- Woosley, S. E. and Bloom, J. S. 2006, ARA&A, 44, 507.
- Woosley, S. E. and Heger, A. 2006, ApJ, 637, 914.
- Woosley, S. E. and Weaver, T. A. 1995, ApJS, 101, 181.
- Zwaan, M. A. and Prochaska, J. X. 2006, ApJ, 643, 675.